



**Duarte Lima Martins**

# **Purification of Complex Biopharmaceuticals with New Processes, Advanced Analytics and Computer-Aided Process Design Tools**

Dissertação para obtenção do Grau de Mestre em  
Biotecnologia

Orientadora : Cristina Peixoto, PhD,  
Senior Scientist,  
ACTU, IBET/ITQB - UNL

Co-orientador : Professor José Paulo Mota,  
Full Professor,  
Requimte/CQFB, FCT - UNL

Júri:

Presidente: Prof. Doutor Carlos A. Salgueiro

Arguente: Professor João G. Crespo

Vogal: Doutora Cristina Peixoto



**FACULDADE DE  
CIÊNCIAS E TECNOLOGIA  
UNIVERSIDADE NOVA DE LISBOA**

**Setembro, 2013**



## **Purification of Complex Biopharmaceuticals with New Processes, Advanced Analytics and Computer-Aided Process Design Tools**

Copyright © Duarte Lima Martins, Faculdade de Ciências e Tecnologia, Universidade Nova de Lisboa

A Faculdade de Ciências e Tecnologia e a Universidade Nova de Lisboa têm o direito, perpétuo e sem limites geográficos, de arquivar e publicar esta dissertação através de exemplares impressos reproduzidos em papel ou de forma digital, ou por qualquer outro meio conhecido ou que venha a ser inventado, e de a divulgar através de repositórios científicos e de admitir a sua cópia e distribuição com objectivos educacionais ou de investigação, não comerciais, desde que seja dado crédito ao autor e editor.



*à minha família*



# Acknowledgements

I would like to thank some people who supported and contributed to the work presented in this MSc thesis, particularly:

To Dr. Cristina Peixoto, my supervisor, for her scientific guidance, remarkable work ethic, confidence and encouragement. I'm deeply thankful for the outstanding people manager that you are, ensuring the highest quality of this work at all stages.

To Professor Paulo Mota, my co-supervisor, for his enthusiasm and enlightening talks on chromatography.

To Professor Paula Alves, for being the demanding and caring head of the ACTU and iBET always pushing the standards; and of course for the opportunity to develop my MSc thesis work at such a stimulating research group.

To Professor Manuel Carrondo, for his inspiring role model of leadership and scientific work.

To Sartorius Stedim Biotech, especially to Dr. Tobias Schleuss, Dr. Franziska Jonas and Dr. Louis Villain, for providing the materials, support and advice throughout this work; and for the opportunity to attend the European Downstream Technology Forum at Sartorius College.

To the funding from *Fundação para a Ciência e a Tecnologia* (PTDC/EBB-BIO/119501/2010) for supporting the work presented in this thesis.

To Pier, for being a great colleague always up for interesting discussions about purification, his pragmatic view on biopharmaceutical industry and for all the laughs!

To Carina Silva, for the patience and experience shared when teaching me all about adenovirus production and handling.

To all my colleagues of the virus lab at ACTU, for all the help as well as for the fun moments; you guys made wearing two lab coats and two gloves fun!

To all former and current colleagues at the ACTU, especially Nuno, Fabiana, Marco, Carina, João and Marcos, for all the assistance, advice, companionship and good work environment.

À Lídia pela compreensão e ânimo em todos os momentos, pelo exemplo de trabalho e resiliência. Por completares o outro lado, um obrigado muito especial.

Aos meus pais que acreditaram sempre em mim e me deram a liberdade de fazer o que gosto. Ao meu irmão por ser um exemplo extraordinário de carácter e determinação. Sem o vosso apoio este trabalho não seria possível.



# Abstract

---

Viruses are highly efficient vectors that have been used for vaccination and gene therapy applications. However, their complexity renders downstream process particularly challenging since devices and strategies especially designed for virus purification are still lacking or need further optimization. After an introduction to the challenges of virus purification and the current strategies being employed, this dissertation presents the study of three different stages of the downstream process: clarification, ultrafiltration and chromatography.

A novel clarification procedure based on diatomaceous earth was evaluated. Small-scale batch incubations led to the identification of Divergan RS – a synthetic non-charged material – as the most promising candidate for integration in a scalable filtration set-up.

Ultrafiltration was addressed with the evaluation of cassette and hollow fiber modules. The results obtained show that cassette module with cut-offs in the 500 kDa range and highly hydrophilic materials enable complete recovery of infective Adenovirus while reducing process time in half when compared with the best hollow fibers. Despite the encouraging results with Adenovirus, the experiments using Retrovirus resulted in low yields and possible optimization strategies were identified.

Membrane technology was also evaluated as an alternative to the packed-bed chromatography columns. By using a scale-down 96-well device, the impact of ligand density, membrane structure and feed conductivity were evaluated for the purification of Adenovirus by ion exchange chromatography. The hydrogel-grafted membrane with ligand density of  $2.4 \mu\text{mol cm}^{-2}$  operated in bind/elute mode shown the best compromise between yield and purity.

Overall, this thesis contributed to the advancement of virus purification field by exploiting innovative technologies.

**Keywords:** virus purification; clarification; ultrafiltration; membrane chromatography; biopharmaceuticals; innovative technologies.

---



# Resumo

---

Os vírus são vectores altamente eficientes que tem sido aplicados para vacinação e terapia génica. Contudo, a sua complexidade torna o processo de purificação particularmente desafiante uma vez que materiais e estratégias desenhadas especificamente para purificação de vírus são inexistentes ou precisam de ser optimizados. Após uma introdução sobre os desafios relativos à purificação de vírus e estratégias atualmente usadas, é apresentado o estudo de três etapas diferentes do processo de purificação: clarificação, ultrafiltração e cromatografia.

Foi estudado um inovador processo de clarificação que usa terras de diatomáceas. Os ensaios em pequena escala identificaram Divergan RS – um material sintético não carregado – como o candidato mais promissor para a integração no passo de clarificação.

Relativamente à ultrafiltração, foram testados vários módulos de cassete e de fibras ocas. Os resultados obtidos indicam que os módulos de cassete com um *cut-off* próximo de 500 kDa e material altamente hidrofílico permitem recuperar 100 % dos Adenovírus infecciosos e ao mesmo tempo reduzir o tempo de processamento para metade relativamente aos módulos de fibras ocas. Apesar dos resultados positivos obtidos com Adenovírus, os ensaios com Retrovírus resultaram em baixos rendimentos e as possíveis causas foram identificadas.

A tecnologia de membrana foi estudada como alternativa à de cromatografia de leito compactado. Através um dispositivo de 96 poços, o impacto da densidade de ligando, da estrutura da membrana e da condutividade da carga foram avaliados na purificação de Adenovírus por cromatografia de troca iónica. A membrana modificada com hidrogel e uma densidade de ligando de  $2.4 \mu\text{mol cm}^{-2}$  resultou no melhor compromisso entre rendimento e pureza.

Na globalidade, esta tese contribuiu para o avanço na área da purificação de vírus através do estudo de tecnologias inovadoras.

**Palavras-chave:** purificação de vírus; clarificação, ultrafiltração; cromatografia de membrana; biofármacos; tecnologias inovadoras.

---



# Contents

<b>I</b>	<b>Introduction</b>	<b>1</b>
<b>1</b>	<b>Purification of complex biopharmaceuticals</b>	<b>3</b>
1.1	Complex biopharmaceuticals . . . . .	3
1.1.1	The challenges of complex biopharmaceuticals . . . . .	3
1.1.2	The Adenovirus - a stable proteic capsid particle . . . . .	6
1.1.3	The Retrovirus - a labile enveloped particle . . . . .	7
1.2	Current scalable DSP strategies . . . . .	8
1.2.1	Harvest . . . . .	9
1.2.2	Clarification . . . . .	10
1.2.3	Concentration . . . . .	11
1.2.4	Intermediate purification . . . . .	12
1.2.5	Polishing . . . . .	13
1.3	Scope of the thesis . . . . .	13
<b>II</b>	<b>MATERIALS AND METHODS</b>	<b>15</b>
<b>2</b>	<b>Materials and Methods</b>	<b>17</b>
2.1	Cell lines, culture media and virus strains . . . . .	17
2.2	Virus production . . . . .	18
2.2.1	Ad5 stock production . . . . .	18
2.2.1.1	CsCl gradient purification . . . . .	18
2.2.2	Ad5 bioreactor production . . . . .	18
2.2.3	RV production . . . . .	19
2.3	Virus purification . . . . .	19
2.3.1	Harvest and Clarification . . . . .	19
2.4	Body feed filtration . . . . .	19

2.5	Ultrafiltration studies . . . . .	20
2.6	Membrane chromatography . . . . .	23
2.7	Analytical methods . . . . .	23
2.7.1	Total virus particles quantification . . . . .	23
2.7.2	Infectious virus particles titration . . . . .	23
2.7.3	DNA quantification . . . . .	24
2.7.4	Protein analysis . . . . .	24
<b>III</b>	<b>RESULTS AND DISCUSSION</b>	<b>27</b>
<b>3</b>	<b>Body Feed Filtration</b>	<b>29</b>
3.1	Virus recovery . . . . .	29
3.2	Impurity removal . . . . .	31
3.3	Discussion . . . . .	32
<b>4</b>	<b>Ultrafiltration</b>	<b>33</b>
4.1	R&D prototypes . . . . .	33
4.1.1	Hydraulic permeability . . . . .	33
4.1.2	Virus recovery . . . . .	34
4.1.3	Impurity removal . . . . .	35
4.1.3.1	Protein clearance . . . . .	35
4.1.3.2	DNA clearance . . . . .	36
4.1.4	Productivity analysis . . . . .	36
4.1.5	Flux Recovery . . . . .	37
4.2	Commercial/pilot production devices . . . . .	38
4.2.1	Hydraulic permeability . . . . .	38
4.2.2	Virus recovery . . . . .	39
4.2.3	Impurity removal . . . . .	40
4.2.3.1	Protein clearance . . . . .	40
4.2.3.2	DNA clearance . . . . .	41
4.2.4	Productivity analysis . . . . .	42
4.2.5	Flux Recovery . . . . .	42
4.3	Discussion . . . . .	43
<b>5</b>	<b>Membrane chromatography</b>	<b>47</b>
5.1	Hydrogel-grafted membranes . . . . .	47
5.1.1	Virus recovery . . . . .	47
5.1.2	Impurity removal . . . . .	48
5.1.2.1	Protein clearance . . . . .	48
5.1.2.2	DNA clearance . . . . .	49
5.2	Directly grafted membranes . . . . .	50
5.2.1	Virus recovery . . . . .	50
5.2.2	Impurity removal . . . . .	51

5.2.2.1	Protein clearance . . . . .	51
5.2.2.2	DNA clearance . . . . .	51
5.3	Discussion . . . . .	52
<b>IV</b>	<b>CONCLUSIONS</b>	<b>55</b>
<b>6</b>	<b>General Discussion and Conclusion</b>	<b>57</b>
6.1	Debottlenecking the DSP rigth from the beginning . . . . .	57
6.2	Future work and outlook . . . . .	58
	<b>APPENDIX</b>	<b>73</b>





# List of Figures

1.1	Structure of the Adenovirus by cross-section representation. . . . .	6
1.2	Structure of the Retrovirus by cross-section representation. . . . .	7
2.1	Schematic representation of the hydrogel-grafted and directly grafted membrane. . . . .	23
3.1	TP recovery after incubation with different filter aids. . . . .	30
3.2	IP recovery after incubation with different filter aids. . . . .	30
3.3	DNA clearance after incubation with different filter aids. . . . .	31
3.4	HCP clearance after incubation with different filter aids. . . . .	32
4.1	NWP <sub>20°C</sub> for the different R&D UF prototypes . . . . .	33
4.2	TP recovery for the different R&D UF prototypes . . . . .	34
4.3	HCP clearance for the different R&D UF prototypes . . . . .	35
4.4	SDS-PAGE comparative analysis of the different R&D UF prototypes . . . . .	36
4.5	DNA clearance for the different R&D UF prototypes . . . . .	36
4.6	Permeate flux and throughput capacity of each R&D UF prototypes . . . . .	37
4.7	Flux recovery for the different R&D UF prototypes . . . . .	38
4.8	NWP <sub>20°C</sub> for the different UF devices . . . . .	38
4.9	TP recovery for the different UF devices . . . . .	39
4.10	HCP clearance for the different UF devices . . . . .	40
4.11	SDS-PAGE comparative analysis of the different UF devices . . . . .	41
4.12	DNA clearance for the different UF devices . . . . .	42
4.13	Permeate flux and throughput capacity of each UF devices . . . . .	43
4.14	Flux recovery for the different UF devices . . . . .	44
5.1	TP recovery for the hydrogel-grafted membrane. . . . .	48
5.2	Protein clearance for the hydrogel-grafted membrane. . . . .	49
5.3	DNA clearance for the hydrogel-grafted membrane. . . . .	49
5.4	TP recovery for the directly grafted membrane. . . . .	50
5.5	Protein clearance for the directly grafted membrane. . . . .	51

5.6	DNA clearance for the directly grafted membrane. . . . .	52
5.7	Experimental design space for the hydrogel-grafted membranes. . . . .	52
A1	Amount of the different filter aids used in dry state. . . . .	75
A2	Volume filed by the wet filter aid with 50 mL of virus bulk. . . . .	75

# List of Tables

1.1	Specifications for biotechnological products. . . . .	5
2.1	Membrane characteristics and feed flow rates used. . . . .	22
4.1	IP recovery for the different R&D UF prototypes . . . . .	34
4.2	IP recovery for the different UF devices . . . . .	40



# List of Symbols

## ACRONYMS

Ad5	Adenovirus serotype 5
ATCC	american type culture collection
BFF	body feed filtration
CEX	cation exchange chromatography
cGMP	current good manufacturing practices
CIP	cleaning-in-place
D-PBS	Dulbecco's phosphate-buffered saline
DE	diatomaceous earth
DF	diafiltration
DMEM	Dulbecco's Modified Eagle Medium
EMA	European Medicines Agency
FDA	Food and Drug Administration
GaLV	gibbon ape leukemia virus
GFP	green fluorescent protein
HEPES	2-[4-(2-hydroxyethyl)piperazin-1-yl]ethanesulfonic acid
HF	hollow fiber
HPV	human papillomavirus
mAb	monoclonal antibody
MF	microfiltration
MLV	murine leukemia virus
MWM	molecular weight marker
PES	polyethersulfone
pI	isoelectric point
PS	polysulfone
PVDF	polyvinylidene fluoride

RC	regenerated cellulose
RV	retrovirus
SDS-PAGE	sodium dodecyl sulphate polyacrylamide gel electrophoresis
SEC	size exclusion chromatography
SEM	standard error of the mean
TFF	tangential flow filtration
TRIS	tris(hydroxymethyl)aminomethane
UF	ultrafiltration
VLP	virus-like particle

## GREEK SYMBOLS

$\dot{\gamma}_w$	shear rate ( $\text{s}^{-1}$ )
$\eta$	dynamic viscosity ( $\text{Pa s}$ )
$\sigma$	conductivity ( $\text{mS cm}^{-1}$ )
$\tau$	throughput capacity ( $\text{L m}^{-2} \text{ h}^{-1}$ )

## ROMAN SYMBOLS

$A$	area ( $\text{m}^2$ )
$C$	concentration
$h$	flow channel height in a cassette module (m)
$J$	flux ( $\text{LMH} \equiv \text{L m}^{-2} \text{ h}^{-1}$ )
$K$	hydraulic permeability (m)
$n$	number of fibers in a hollow fiber module
$Q$	volumetric flow rate ( $\text{mL min}^{-1}$ )
$r$	radius (m)
$Re$	Reynolds number (–)
$t$	time (min)
$v$	linear velocity ( $\text{m s}^{-1}$ )
$w$	flow channel width in a cassette module (m)
$Y$	recovery yield (%)
$g$	gravitational acceleration at the Earth's surface ( $9.81 \text{ m s}^{-2}$ )
Abs	absorbance (AU)
CF	concentration factor (–)
Da	molecular mass ( $\text{Dalton} \equiv \text{g mol}^{-1}$ )
DNA	deoxyribonucleic acid ( $\mu\text{g mL}^{-1}$ )
HCP	host cell protein ( $\mu\text{g mL}^{-1}$ )
IP	infectious particles ( $\text{particles mL}^{-1}$ )
$\text{NWP}_{20^\circ\text{C}}$	normalized water permeability corrected for $20^\circ\text{C}$ ( $\text{LMH bar}^{-1}$ )
P	pressure (bar)
rpm	rotations <i>per</i> minute ( $\text{min}^{-1}$ )

T	temperature ( $^{\circ}\text{C}$ )
TCF	temperature correction factor ( – )
TMP	transmembrane pressure (bar)
TP	total particles (particles $\text{mL}^{-1}$ )
WCW	wet cell weight ( $\text{g L}^{-1}$ )

# **SUBSCRIPTS AND SUPERSSCRIPTS**

$f$	feed
$i$	initial
$p$	permeate
$r$	retentate





# Part I

## Introduction





# Purification of complex biopharmaceuticals

## 1.1 Complex biopharmaceuticals

Biopharmaceuticals are structured and highly specific biomolecules capable of targeting unmet medical needs where other drugs have failed. The success of these novel bio-based pharmaceuticals has been reshaping medical therapies over the past decades<sup>[1]</sup>. Nowadays there are numerous biopharmaceuticals (both approved and under development) with a wide range of sizes, levels of complexity and medical indications<sup>[2,3]</sup>. Some examples of approved biotherapeutics are the Factor VIII (blood factor), tissue plasminogen activator (anticoagulant/thrombolytic), insulin and insulin-derived products, erythropoietins, interferon- $\alpha$ , pegaptanib (nucleic acid-based anti-angiogenic medicine), monoclonal antibodies (mAbs), human papillomavirus (HPV) virus-like particle (VLP) vaccine, inactivated influenza virus vaccines and adeno-associated viral (AAV) gene therapy vector (Glybera<sup>®</sup>)<sup>[2,4]</sup>.

Among the above-referred biomolecules virus-based biopharmaceuticals hold a great promise to redefine modern medicine in different fields such as vaccination<sup>[5]</sup>, gene therapy<sup>[4]</sup> and cancer treatment<sup>[6]</sup>. However these biopharmaceuticals represent also a series of the challenges both product- and process-wise since their are not as well studied and developed as other less complex biopharmaceuticals already established.

### 1.1.1 The challenges of complex biopharmaceuticals

Virus and virus-like particle are considerably larger than an insulin protein or a mAb and their size can range from 20 nm (parvovirus) to 300 nm (Measles and Mumps virus),

with different possible morphologies (*i. e.* the rod-shape of Baculovirus)<sup>[7,8]</sup>. The highly repetitive tri-dimensional structure is fundamental for immunization in the case of vaccines. Additionally, *post*-translational modifications, like glycosylation, impact the immunogenicity and antigenicity of the vaccine<sup>[9,10]</sup>. For gene therapy applications the vector quality is crucial<sup>[11]</sup>.

As a result of this complexity, animal cell lines have to be used often for production of these virus-based biopharmaceuticals. The new virus vaccines are now produced in cell-based systems. The traditional production with fertilized eggs has several drawbacks since it is a work-intensive process, is dependent on egg supply, is not fast enough in the case of a global pandemics and might cause anaphylactic reactions due to egg's proteins<sup>[1,7,12]</sup>. Vaccines recently developed and under development make use of continuous mammalian cell lines such as the African green monkey kidney (VERO) cells<sup>[13,14]</sup>, the human lung fibroblast (MRC-5) cells<sup>[15]</sup>, Madin-Darby Canine Kidney (MDCK) cells<sup>[16]</sup>, human embryonic retina-derived PER.C6<sup>®</sup> cells (Crucell)<sup>[17–19]</sup> and human embryonic kidney (HEK) 293<sup>[19,20]</sup>.

The VLP-based vaccines might be produced by a wide range of hosts from mammalian cell lines to transgenic plants, however only VLPs produced in yeast and animal cell lines were approved by regulatory authorities<sup>[5,8]</sup>. The recombinant hepatitis B vaccines are produced almost exclusively in yeast systems (*Saccharomyces cerevisiae*, *Pichia pastoris* and *Hansenula polymorpha*) with the exception of chinese hamster ovary (CHO) cells, which is the only mammalian cell line used. *S. cerevisiae* is also used for production of the Merck & Co's HPV-VLP<sup>[21]</sup> whereas the GSK's HPV-VLP is produced with the baculovirus-insect cell (B-IC) system<sup>[22]</sup>. These expression systems seem to have a favorable compromise between high productivity/yield and capability to perform *post*-translational modifications<sup>[5]</sup>.

Contrarily to VLPs, the gene therapy vectors are less flexible in terms of production system and the system chosen is dependent on the virus used. Ad-based vectors are produced in a complementing cell line (see Section 1.1.2), such as the 293 and the PER.C6<sup>®</sup> cell lines<sup>[19,23]</sup>. In the case of AVV vectors, like UniQure's Glybera<sup>®</sup> – recently approved by EMA –, these can be produced in mammalian cell lines as well as with the B-IC system<sup>[24,25]</sup>. The current retrovirus production systems rely on genetically engineered virus packaging cell lines (see Section 1.1.3), usually human-derived cell lines<sup>[26,27]</sup>.

As biopharmaceuticals are intended for therapeutic human use there are stringent guidelines put in place by the regulatory agencies (*e. g.* EMA or FDA). The Table 1.1 reports the quality attributes evaluated by the regulatory authorities<sup>[28,29]</sup>.

The analyticals for virus-based biopharmaceuticals must be highly specific and robust, however often new analytical assays must be developed and validated, specially for innovative therapeutic biomolecules. Additionally, the lack of well-characterized and accepted standards adds up to the challenges of developing new analytical assays for such specific products<sup>[1,31]</sup>.

The final goal is to obtain a biopharmaceutical of high **purity** (process-related impurities, like HCP and DNA, within regulatory specifications), high **potency** (highest concentration feasible of the relevant active component) and high **quality** (low concentration of product-derived impurities relatively to the desired product, *e. i.* virus capsid proteins or non functional virions).

Table 1.1: Specifications for biotechnological products<sup>[28–30]</sup>.

Attribute	Specification
Appearance and description	Color Physical state Clarity/turbidity (Qualitative statement)
Identity	Multiple tests might be required: Physicochemical Biological immunichemical (Highly specific but might be qualitative)
Purity	
Product-related impurities	Degradated product Truncated forms Molecular variants Aggregates
Process-related impurities	Host cell protein (HCP) Host cell DNA Media components/ancillaries Enzymes/chemicals Leachables
Potency	Cell-based test <i>or</i> Animal-based test
Quantity	Protein mass <i>or</i> Potency (if applicable)
Safety	Sterility Adventitious virus Endotoxins/Pyrogens Mycoplasma
General	pH Osmolarity

Two highly relevant representatives of these virus-based biopharmaceuticals are adenovirus and retrovirus.

### 1.1.2 The Adenovirus - a stable proteic capsid particle

The *Adenoviridae* family is composed of over 100 virus, 57 serotypes of which are capable of infecting humans<sup>[32]</sup>.

The adenovirus serotype 5 (Ad5) was the first adenovirus discovered when its icosahedral shape was revealed by Horne in 1959<sup>[33]</sup>. Since then it has been extensively studied, used as virus model and nowadays is widely characterized. The Ad5 is a nonenveloped double-stranded DNA virus with a molecular weight of 150-170 MDa (90-100 nm in diameter)<sup>[32,34,35]</sup>, has a pI of approximately 4.5 and thus is negatively charged at physiological pH<sup>[36]</sup>. The virus is composed of 11 different proteins (Figure 1.1), 7 are the structural proteins (II, III, IIIa, IV, VI, VIII and IX) which compose the icosahedral virus capsids and the remaining 4 proteins (V, VII, mu and terminal protein) are packed inside the capsid together with the virus DNA to form the core<sup>[32,37,38]</sup>.

The virus capsid is composed of twelve hexon trimers (polypeptide II - 107.9 kDa for Ad5) in each of the 20 facets and twelve pentons in each of the twelve vertices (Figure 1.1). Each penton is a protein composed of one pentamer, the penton base (polypeptide III - 63.3 kDa for Ad5), and one trimer, the fiber (polypeptide IV - 61.6 kDa for Ad5) which is responsible for the adsorption to the cell surface via the CAR (Coxsackie/Adenovirus receptor) and  $\alpha$ v-integrins. The remaining (minor) coat proteins are involved in virus stability, correct assemble and disassemble of the virion<sup>[32,38,39]</sup>.

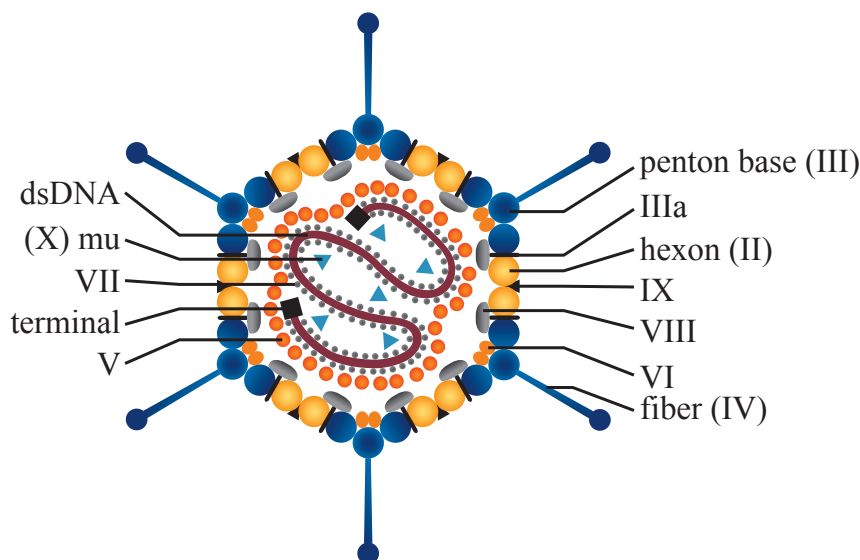


Figure 1.1: Structure of the Adenovirus by cross-section representation. The coat proteins are listed on the right side and the core proteins and DNA are on the left side.

The application of Ad5 goes beyond fundamental research and its use as biotechnology product is very significant, either as gene therapy vector<sup>[40]</sup>, oncolytic virus<sup>[41]</sup> or recombinant vaccines<sup>[42,43]</sup>. The best know examples are the use of recombinant p53-Ad5 approved in China for cancer therapy<sup>[44,45]</sup> and the Merck & Co's candidate HIV Ad5-based vaccine

(although clinical tests failed for Ad5-based vaccine, currently different, rarer Ad serotypes are being evaluated)<sup>[46,47]</sup>.

However to use Ad-based therapies safely, these virus are genetically modified to render replication-incompetent vectors (or conditionally replication-competent virus for oncolytic therapy). To accomplish this several genes of the Ad5 genome were removed or mutated. Initially the genes targeted were involved in viral DNA transcription, inhibition of cell apoptosis, avoiding host immune response and viral DNA replication<sup>[32]</sup>. More recently, helper-dependent Ad (also named gutless or high-capacity) were developed. Since these vectors have no viral DNA, a helper virus has to be used to provide all structural proteins<sup>[23,32,48,49]</sup>.

For the production of replication-incompetent adenoviral vectors *trans*-complementing cell lines must be used in order to provide the deleted functions. Several cell lines have been used for Ad production, with the 293 and the PER.C6<sup>®</sup> being the most used. Since the Ad-producing cell lines can adapted to grow in suspension, stirred-tank bioreactors have been used with or without the aid of microcarriers<sup>[19,23]</sup>.

### 1.1.3 The Retrovirus - a labile enveloped particle

The *Retroviridae* is a family of viruses characterized by their RNA genome and its retro-transcription into DNA prior to protein synthesis. Notable species of this family include the murine leukemia virus (MLV), belonging to the *gamma-retrovirus genus* (herein referred to as retrovirus (RV)) and the human immunodeficiency virus (HIV) which belongs to the *Lentivirus genus*<sup>[50]</sup>. The RV is an enveloped, spherical, slightly pleomorphic particle with a diameter of 100-120 nm (Figure 1.2). The virion structure is divided in three major parts, the

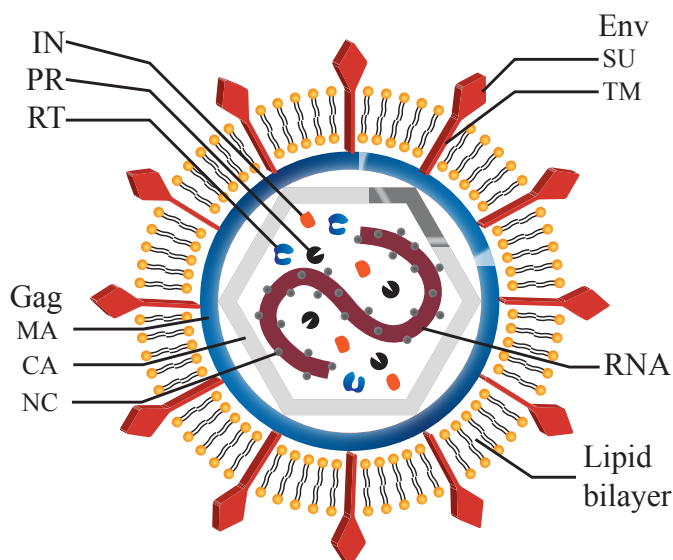


Figure 1.2: Structure of the Retrovirus by cross-section representation.

envelope, the proteic capsid and the viral genome. The envelope that covers the the proteic capsid is composed by a bi-lipidic layer and 100-300 Env glycoproteins (69.8 kDa) consisting of transmembrane (TM, 19.9 kDa) and surface (SU, 47.9 kDa) subunits. The SU subunit interacts with the cell membrane receptors to promote the fusion of the envelope with the cell membrane during the infection process. Given its function, the Env protein (and the virus

envelope) is of great relevance of highly infective retroviral preparations. The Gag protein (60.7 kDa) interacts both with the Env proteins by its N-terminal matrix domain (MA) and the inner space of the virus capsid with through its C-terminal nucleocapsid (NC) domain. Inside this proteic structure, besides the ssRNA molecule, there are also the PR (responsible from virus' protein cleavages during assembling, budding and maturation), the RT (which does the reverse-transcription of the viral RNA) and the IN (responsible for integrating the pro-viral DNA) proteins<sup>[51,52]</sup>.

Retroviral vectors are highly advantageous for gene therapy due to their high transduction efficiency of replicating cells, low immunogenicity and ability to integrate the proviral cDNA (with the therapeutic gene) into the host genome, rendering a long-term effect<sup>[48]</sup>. Moreover, RV are the second most used gene therapy vector in clinical trials worldwide (the first being adenovirus)<sup>[53]</sup>.

Since retrovirus have a modular structure they can be pseudotyped, *i. e.* the *env* region of the genome can be replaced by the *env* region of another, more favorable, retrovirus. The possibility to engineer the vector allowed to change, restrict ou broaden vector tropism and to modulate its immunogenicity. Among several Env proteins used, the MLV-based retrovirus pseudotyped with gibbon ape leukemia virus (GaLV) Env has been one of the most studied<sup>[26,27]</sup>.

As earlier described for Ad5, also retroviral vectors being developed for human therapeutic purposes must be replication-incompetent. This is accomplished by providing the transgene of interest together with the packing signal in a different transcriptional unit(s) than the packing functions (*env* and *gag-pro-pol*). Current RV generations have three different transcriptional units (*transgene*, *gag-pro-pol* and *env*) with reduced sequence homology, thus reducing greatly the frequency of replication-competent RVs<sup>[26,27]</sup>.

For retrovirus production the packing functions (*i. e.* structural proteins) can be supplied either by a plasmid transfection (transient production) or by a packing cell line engineered to express constitutively those functions (stable production). While transient production is only suitable for small scale research purposes, the stable production includes the long process of developing a high titer packing cell line but yields a continuous low-variability production suitable for clinical lots. Currently, human cell lines, namely HEK-derived, are preferred to the murine cell lines for the development of retrovirus-producing cells<sup>[26,27,54]</sup>.

The RV-packing cells are generally cultured in static systems due to their anchorage-dependent feature. High capacity static system such as the Cell Factory<sup>®</sup> have been reported for clinical production of RV under current good manufacturing practices (cGMP)<sup>[55–57]</sup>. These kind of strategies enable a limited but rapid and reliable scale-up and might provide enough material for pre-clinical and early clinical phases.

## 1.2 Current scalable DSP strategies

The biopharmaceutical process is no longer seen as the sum of upstream with downstream processes and there is a effort to integrate and design together production and purification. Despite this, the downstream process is still crucial to obtain the final intended product; also the substantial developments achieved in the upstream process were not matched by small



improvements in the downstream. Furthermore, the cost of purification can go from 50 % up to 70 % of the total process<sup>[58,59]</sup>. Meaning that careful choice of operations, materials and equipment should be made in order to keep the whole process cost-effective. Besides cost, the scalability of the DSP developed is a key issue. Robustness is also a required feature so that small variations in upstream processing as well as in previous downstream operations do not impact the whole bioprocess performance and final product quality.

The following section describe the state-of-the-art regarding virus purification including novel technological advances, emerging industry trends and rational process development approaches for different stages of the DSP train. Some examples are the greater integration between upstream and downstream, high density cell systems, continuous processing, scale-down tools closed systems, modulatory, numbering up instead of scale-up (for niche biopharmaceuticals) and disposable technologies<sup>[60–64]</sup>.

### 1.2.1 Harvest

The first steps of the purification train are heavily influenced by the bioreactor bulk features, namely cell density, cell viability or if the product is secreted for the culture supernatant or if the cells have to be lysed.

In cases such as Ad5 production, is usually chosen to recover both the intra- and extra-cellular virus fraction and thus an additional step is performed for virus release<sup>[19,23]</sup>. The cell lysis can be performed using different methods such as freeze-thaw, detergents, French Press, homogenizer or sonication<sup>[65]</sup>. Among these, non-ionic detergents especially Triton™ X-100 have been preferred<sup>[18,19,65–67]</sup>. Incubating the bulk with detergent is efficient, fast, robust, easily scalable, cost-effective and does not require any investment in equipment, however removal of this additive has to be confirmed.

Although cell lysis enables the recovery of intra-cellular virus it also releases the host cell DNA and protein which should be removed from the final product. Host cell DNA is of special concern because it increases substantially bulk viscosity but also due to regulatory requirements. The DNA acceptable levels set by the regulatory authorities are generally between 10 ng and 10 pg *per* dose, depending on type of product, medical indication, production host and administration route. Therefore, the majority of scientific manuscripts published and patents disclosed refer an incubation step with nuclease (*e. g.* Benzonase®) either simultaneously with cell lysis or after clarification<sup>[18,19,65–68]</sup>. For enveloped virus, like RV or baculovirus, cell lysis is not required since the virus are secreted by the producer cells – budding process. Therefore, the use of nuclease might be avoided for enveloped virus DSP due to its high costs<sup>[54,69]</sup>.

Selective precipitation has been suggested as an alternative to nuclease treatment to remove host cell DNA<sup>[17,70–72]</sup>. Cationic detergents (namely domiphen bromide) are able to precipitate DNA as well as Ad particles (both negatively charged and mildly hydrophobic). However fine adjustment of precipitant concentration enables up to 90 % DNA removal with more than 90 % Ad recovery<sup>[70]</sup>. Selective DNA precipitation has the advantage of being inexpensive, easily scalable (precipitated DNA can be removed by depth filter) and suitable for high cell density processes<sup>[17,71]</sup>.

### 1.2.2 Clarification

The goal of clarification is to recover and stabilize the product while removing solids, cells/cell debris and process impurities (DNA and HCP). Centrifugation and membrane filtration are the two common choices for the initial clarification.

Centrifugation is an operation widely used at laboratory scale for research purposes both to clarify the cell culture fluid (CCF) and to obtain high purity viral preparations (by CsCl gradient ultracentrifugation). The centrifugal separation is based on the solutes' different densities meaning that clarification is generally a fast process. However, centrifugation has several issues like the high maintenance costs, the lack of reliable scale-down model, does not remove soluble impurities and safety risks must be considered (for instance the Ad5 forms aerosols)<sup>[19,68,73]</sup>. Despite the earlier described limitations, continuous flow centrifugation are quite common in current industrial-scale operations for mAbs clarification where bioreaction yields very high cell density CCFs ( $10^7$  cell mL<sup>-1</sup> and above). However in these cases the clarification also comprises a depth filter operation to achieve higher removal of soluble impurities (DNA and HCP) and low turbidity<sup>[74–77]</sup>.

Microfiltration (MF) is an alternative to centrifugation which can be easily scaled up and implemented in a cGMP setting. Microfiltration membranes have pore sizes in the 0.1–10 µm range and can be classified as depth filters or "regular" filter depending on whether the solids are retained throughout filter matrix/medium or only at its surface, respectively. Additionally, depth filter might include filter aids, *e. g.* diatomaceous earth (DE), to modify its structure and charge<sup>[78]</sup>. Depth filters have been used for a wide variety of VLPs and viruses (enveloped and non-enveloped) with recovery yields of approximately 90 %<sup>[66,67,69,79,80]</sup>. Depth filters are usually preferred for feed streams with high biomass contents, sometimes lysed CCF, due to their ability to remove solids and impurities by different mechanisms (size exclusion, hydrophobic and electrostatic interactions)<sup>[81]</sup>. Carefull selection of the filter (pore size, filter material, number and sequence of filter units) and operation parameters (inlet flow rate, pressure drop, conductivity and pH) must be assessed in order to avoid virus losses and to allow solids and soluble impurities retention throughout the whole depth of the filter medium rather than only at the filter surface. Often the trade-off between feed flow rate/throughput and filter capacity/impurity removal should be evaluated<sup>[77,82]</sup>.

Membrane microfiltration has also been performed either in normal (dead-end) or tangential flow filtration (TFF)<sup>[79,83]</sup>. Microfiltration is usually operated at low pressures, especially TFF (less than 0.7 bar), and is better suited for low cell density CCFs<sup>[74]</sup>. However, membrane fouling or shear stress-induced cell lysis can become an issue<sup>[84]</sup>.

More recently, a new microfiltration separation was purposed where a filter aid is mixed with the CCF instead of being incorporated in the depth filter units<sup>[85,86]</sup>. The CCF and filter aid (diatomaceous earth, layered double hydroxides or synthetic materials) are mixed and fed to a microfilter. This novel filtration would permit an enhanced adsorption during mixing and the formation of highly porous and highly permeable cake (body feed) supported by the filter aid, similarly to what is done in the brewing industry where diatomaceous earth is used to clarify beer<sup>[87]</sup>. Several patents applications claim that the body feed filtration (BFF) would avoid membrane fouling, enable lower pressure operation for longer times at

higher flow rates without compromising impurity removal. One paper recently published<sup>[88]</sup> refers the use of DE for clarification of a poliovirus CCF, however the performance of this method was not disclosed and its potential remains unexplored.

### 1.2.3 Concentration

Large-scale process can produce high volumes of CCF (up to 20 kL for mAbs<sup>[89]</sup>) which must be concentrated 10–100 times to be further purified by chromatographic steps. Ultrafiltration (UF) is a pressure-driven separation which employs anisotropic membranes with molecular weight cut-offs (MWCO) ranging from 0.5 to 1000 kDa<sup>[84]</sup>. (The MWCO is defined by the solutes' molecular mass which are 90 % retained by the membrane.) These membranes can be constructed with different polymers like regenerated cellulose (RC), polysulfone (PS), polyethersulfone (PES) and polyvinylidene fluoride (PVDF), although RC and modified RC displays better trade-off between low (unspecific) protein binding, mechanical strength and resistance to cleaning procedures (chemical agents and temperature)<sup>[74,90,91]</sup>. Ultrafiltration membrane are generally composed by two main layers, a thick macroporous structure provides mechanical strength while a thin skin layer is responsible for membrane selectivity and permeability<sup>[74]</sup>.

Ultrafiltration is usually performed in TFF mode where the cross flow at the membrane surface creates a "sweeping action" that avoids or lessens concentration polarization and gel layer formation. UF processes are usually performed at constant transmembrane pressure (TMP, see equation 2.5, page 20), however constant permeate flux or constant permeate pressure operation are also feasible<sup>[74]</sup>. Ultrafiltration has been widely used both in concentrative mode as well for buffer exchange (diafiltration, DF) step and is present in almost every virus DSP described in the literature<sup>[79,83,92–97]</sup> and patents disclosed<sup>[18,71,98]</sup>. The membranes used in virus UF have MWCO in the range of 100–750 kDa allowing for high virus recovery (70–100 %). The TMP generally used is between 0.5 and 1.4 bar but the optimum cross flow can vary greatly due to different structural stability of virus; enveloped virus are more labile than non-enveloped virus and thus more prone to shear-induced damage<sup>[83,97]</sup>. The membrane modules might be constructed in different arrangements, for example flat sheet cassette and hollow fibers. However the majority of the reports published refers the use of hollow fibers (HF) modules for virus processing<sup>[7,99]</sup> due to the fact that HF modules provide wider flow paths resulting in lower shear rates<sup>[7,84]</sup>. Shear rate is proportional to the linear velocity of the feed and inversely proportional to the flow channel diameter or height (see equation 2.9, page 21 for further details). The flow channel geometry influences the shear rate two ways: firstly, the wider flow channel result in lower linear velocity for the same volumetric flow rate; and secondly, the wide flow channel results itself in lower shear rates. Although UF cassettes results in greater shear rates, these modules provide shorter processing times as the flow channel hydrodynamics are more effective than HF in avoiding concentration polarization and gel layer formation<sup>[7,84]</sup>.

Besides UF, rediscovered techniques like aqueous two-phase systems<sup>[100,101]</sup> and precipitation<sup>[102–104]</sup> have been suggested for early-stage operations in mAb DSP, however its applicability and efficacy remains unclear for virus-based biopharmaceuticals<sup>[105]</sup>.

### 1.2.4 Intermediate purification

The purification step(s) employs high resolution unit operations capable of removing impurities closely related with the product, being chromatography the best example. Purification scientists have relied mainly on ion-exchange and size exclusion chromatography to process virus particles<sup>[23,26,92,106]</sup>, although other techniques like affinity<sup>[92,99]</sup>, hydrophobic interaction (HIC)<sup>[107,108]</sup> and multimodal<sup>[67]</sup> have been suggested.

Ion-exchange (IEX) chromatography is the method of choice for capture step. The virus-containing feed is loaded in the chromatographic matrix under low or moderate conductivity and recovered upon a conductivity increase of the mobile phase. The functional groups Q (quaternary amine) and DEAE (diethylaminoethyl) are common choices for this bind/elute (or positive) mode chromatography<sup>[23,99]</sup>. Accurate process development enables highly selective AEX chromatography capable of discriminate between whole virus and virus capsid proteins<sup>[109]</sup> or different adenovirus serotypes<sup>[110,111]</sup>.

Despite being widely used, packed-bed chromatography has several disadvantages: the pressure drop is high and increases during operation due to matrix deformation or pore obstruction; scale-up requires changes in the column geometry making scale-up problematic; the mass transfer is slow since it is limited by pore diffusion; the capacity is limited to the ligand available at bead surface since the small pores (10–400  $\mu\text{m}$ ) will exclude the virus particles. Additionally, the diffusion-limited transport greatly reduces binding capacity at high flow rates (20–500 column volumes *per* hour)<sup>[112–114]</sup>.

Membrane chromatography, in which a macroporous membrane serves as support to bound functional ligands, has the potential to overcome the limitations of the traditional chromatography resins<sup>[114]</sup>. Monoliths – a single polymer block with a network of functionalized flow paths highly interconnected – have also been suggested as an alternative for packed-bed chromatography<sup>[115]</sup>. The nearly-convective mass transport enables operation at flow rates up to 500 membrane volumes *per* hour without decreasing binding capacity – reducing processing times. The wide porous (up to 3  $\mu\text{m}$ ) allow lower pressure drops and compact design compared with packed-bed chromatography reduce hardware requirements and facility footprint. Scale-up is greatly facilitated due to the modular design of chromatography supports. Since membranes adsorbers are single-use devices, column (re)packing, cleaning and validations are avoided. The advantages referred above enable savings with the consumables and labor costs<sup>[62,116,117]</sup>, despite some limitations regarding membrane chromatography. While multilayer membrane modules mitigated the distorted inlet flow, uneven membrane thickness and uneven pore size of the first membrane adsorbers some issues still remain. The major drawback of membrane adsorbers is lower binding capacity compared with packed-bed columns due to the lower surface-to-volume ratio<sup>[113,114]</sup>. AEX membrane adsorbers were first developed as flow-through (negative mode) chromatography for polishing step in mAbs DSP to capture virus, DNA and HCP<sup>[118]</sup>. However when used for virus purification, the product recovery (desorption) and removal of closely related species (*e. g.* DNA) is limited. Considering these drawbacks optimization of ligand density and membrane surface tri-dimensional structure were suggested to overcome the referred limitations<sup>[119]</sup>.

Another different option to improve chromatography is the use of radial columns, where

the chromatographic resin is packed in a cylinder form. The advantage of this columns lie in the radial flow design which enables a small bed length while attaining high column volumes. This feature results in low and uniform pressure drops across the packed-bed allowing for increased flowrates (and productivity), small equipment foot-print and linear scale-up since column geometry is kept<sup>[120,121]</sup>.

Recently, Genzyme and Genentech's scientists have developed a continuous process for purification of mAbs and recombinant therapeutic enzymes using HIC and affinity chromatography<sup>[63,64,122]</sup>. In the conventional batch operation the chromatographic matrix is loaded until product breakthrough is detected at the outlet (*i. e.* 5 or 10 % of feed concentration). This means that only a fraction (between 30 and 70 %) of the chromatographic resin capacity is used because breakthrough happens before the matrix gets fully loaded. In the described periodic counter-current chromatography (PCC) process the breakthrough effluent is loaded onto a second column enabling loading the first column until exhaustion (up to static binding capacity). This strategy enables, reduced buffer consumption, shorter processing times and better matrix usage (with concurrent investment and facility footprint savings)<sup>[63,64]</sup>.

### 1.2.5 Polishing

The final step of purification aims to remove small quantities of impurities and to exchange the buffer for the final formulation. Ultrafiltration and size exclusion chromatography (SEC) have been used for this purpose although ultrafiltration is preferred for large-scale manufacture<sup>[68,71,106]</sup>. Buffer exchange by size exclusion chromatography is performed in way such that virus particles are excluded from the resin while smaller size molecules (buffer, HCP and DNA) and ions are retained<sup>[117]</sup>. However, due to the diffusion-limited fractionation mechanism and compressible nature of SEC resin, low flow rates have to be used thus resulting in low productivity. Furthermore, scale up of SEC is limited by technical and economic constraints<sup>[74,123]</sup>. On the other hand, ultrafiltration is easily scalable and allows for buffer exchange of high volumes. Additionally, some components of formulation buffers (*e. g.* glycerol or trehalose<sup>[124,125]</sup>) that increase the viscosity can be incorporated in diafiltration buffers contrarily to chromatography. However TMP, shear rate, diafiltration number, MWCO and membrane material must be carefully optimized for optimal product recovery and short processing time. Hydrophobic interaction chromatography (HIC) was recently suggested to remove trace amounts of HCP and DNA, however the high conductivity required limits its application to virus sensitive to high conductivity<sup>[107,108,126]</sup>.

## 1.3 Scope of the thesis

Virus are biopharmaceuticals holding a tremendous potential for vaccine and gene therapy applications. Despite recent research efforts have targeted purification of complex biological particles, virus downstream processing is still a challenging field. The product characteristics – virus lability/stability or large size – limit the unit operations that can be used. Furthermore, the upstream process employed results in closely related impurities that have to be removed in order to achieve clinical-grade preparations. Purification devices and strategies

especially designed for virus purification are lacking or need further optimization; additionally most of the research and development (R&D) has been focused on the chromatographic step – considered the major bottleneck of the purification train. As a result, the literature thoroughly evaluating non-chromatographic operations for virus DSP is scarce. This thesis aims to improve the state-of-the-art virus purification by evaluating essential but less studied separations – clarification and ultrafiltration – as well as other better characterized DSP steps – membrane chromatography.

Clarification by depth filter is a technology easily scalable, capable of removing soluble impurities and suspended solids. However limitations such as low filter capacity and low flow rates have been identified<sup>[77,82]</sup>. In Chapter 3 a novel clarification process based on body feed filtration (or cake filtration) concept was evaluated. For this purpose different filter aids (DE and synthetic polymer; charged and non-charged) were assessed for clarification of an Ad5 bioreactor bulk.

Ultrafiltration is present in all large-volume virus purification schemes. Virus concentration and diafiltration is usually performed using hollow fiber UF modules. Despite its generalized use, HF are known to be slower and more prone to fouling when compared with cassette modules. Considering the advantages of cassette UF, a study with R&D UF cassette prototypes was performed in the first part of Chapter 4. In the second part of the chapter, a comparative evaluation between commercial HF and late-stage cassette devices is described. Two different virus (Ad5, non-enveloped, and RV, enveloped) were used as models to characterize membrane MWCO and filter material and its impact on virus recovery, impurity removal and processing time.

Membrane adsorbers have several advantageous features comparing with the traditional packed-bed column chromatography. However, further improvements are required to increase the adoption of this technology. The last part of this thesis (Chapter 5) reports the use of a scale-down tool to evaluate how conductivity of the mobile phase, ligand density and structure of an IEX membrane affect a chromatographic purification of Ad5.

Overall, this thesis aims to evaluate the potential of enhanced and innovative technologies to improve productivity and reduce cost-of-goods in the whole DSP train.

## Part II

# MATERIALS AND METHODS







# Materials and Methods

## 2.1 Cell lines, culture media and virus strains

The 293 cell line (ATCC CRL-1573) was used for adenovirus production as well as infectious virus particles (IP) titration. A recombinant replication-defective adenovirus serotype 5 harboring a transgene for the green fluorescent protein (GFP) were used; the virus stock was kindly provided by Professor Stefan Kochanek, University of Ulm, Germany. The recombinant RV was produced in 293-derived cell line gene genetically engineered to provide constitutively the packing functions required for RV assembly as described elsewhere<sup>[127]</sup>. The RV produced is derived from the murine leukemia virus (MLV) with the Gibbon ape leukemia virus (GaLV) ecotropic envelope and harbors a GFP reporter gene. The 293 T cell line (ATCC CRL-11268) was used for infectious RV titration.

The 293 and 293 T cell lines were grown in cell culture flasks (353112, BD Falcon™, USA) with Dulbecco's Modified Eagle Medium (DMEM, 41966-052, Gibco®, UK) supplemented with 10 % (V/V) Fetal Bovine Serum (FBS, 10270-106, Gibco®, UK). For the 293 Flex GFP the medium used was DMEM without phenol red (31053-036, Gibco®, UK), supplemented with 10 % (V/V) FBS and 4 mM L-Glutamine (25030-024, Gibco®, USA). The 293 cells were grown in a humidified atmosphere of 5 % CO<sub>2</sub> at 37°C, whereas the Flex 293 and 293 T were grown in a 8 % CO<sub>2</sub>. The cells were routinely propagated twice a week using 0.05 % Trypsin-EDTA (25300-104, Gibco®, UK). The cell concentration and viability were determined by counting cells on a Fuchs-Rosenthal haemocytometer (Brand, Germany) using the dye exclusion method with 0.1 % trypan blue (15250-061, Gibco®, UK).

For the suspension culture system (*i. e.* bioreactor production, see section 2.2.2) the 293 cells adapted to suspension were grown with the commercially available serum-free culture medium Ex-Cell 293 (14570C, SAFC®, USA) supplemented with 4 mM L-Glutamine

(25030-024, Gibco<sup>®</sup>, USA). The cells were routinely propagated twice a week using an inoculum of  $0.5 \times 10^6$  cell mL<sup>-1</sup>. Erlenmeyer shake flasks (431255, CORINING, USA) were used for suspension cell culture in a humidified atmosphere of 8 % CO<sub>2</sub> at 37°C. Agitation was provided by orbital shaking at 110 rpm.

## 2.2 Virus production

### 2.2.1 Ad5 stock production

For the small scale virus production, ten 175 cm<sup>2</sup>-cell culture flasks (353112, BD Falcon<sup>™</sup>, USA) with 80-90 % confluence were infected with a previously purified and characterized viral stock using a multiplicity of infection (MOI) of 5.

#### 2.2.1.1 CsCl gradient purification

After 48 h, the infected cells were centrifuged at 1 500 *g* for 5 min, resuspended in lysis buffer (10 mM TRIS, pH 8.0, 0.1 % (V/V) Triton X-100) and vigorously shaken. The cellular debris were removed by centrifugation at 1 000 *g* for 10 min and the virus-containing supernatant was collected. This fraction was further purified by two rounds of CsCl ultracentrifugation (Optima<sup>™</sup> LE-80K, SW 41 Ti rotor both BECKMAN COULTER, USA). The first round consisted in a discontinuous CsCl ultracentrifugation (1.25/1.45 kg/L density) at 151 000 *g* for 90 min. The visible virus band was extracted and processed by a continuous CsCl gradient ultracentrifugation (1.32 kg/L) at 151 000 *g* for 18 h. After the second of ultracentrifugation, the virus band collected was purified by SEC (HiPrep<sup>™</sup> 26/10 Desalting, 17-5087-01, GE Healthcare Life Sciences, Sweden) in order to change for the formulation buffer (10 mM TRIS, pH 8.0, 2 mM MgCl<sub>2</sub>, 0.5 M trehalose). The purified virus stock was sterilized with 0.2 µm filter (4554, Pall, USA), aliquoted and stored at -80°C until further use.

### 2.2.2 Ad5 bioreactor production

The Ad5 production was performed in a 5-L working volume bioreactor (Sartorius Steadim Biotech, Germany). The dissolved oxygen was controlled at 50 % air saturation by a N<sub>2</sub>/O<sub>2</sub>/air mixture delivered by a sparger. The aeration rate was 0.01 vvm (vessel volumes *per* minute). The pH-value was controlled at 7.2±0.05 by aeration with CO<sub>2</sub> in the gas mixture and by base addition (1 M NaHCO<sub>3</sub>). The temperature was controlled at 37°C using an external water-filled jacket. Mixing was provided by two 6-segment Ruston impellers with the agitation rate controlled between 60 and 210 rpm.

The bioreactor inoculum was  $0.5 \times 10^6$  cell mL<sup>-1</sup>, the cell concentration at infection (CCI) was  $1 \times 10^6$  cell mL<sup>-1</sup> and a MOI of 5 was used. The bioreactor was harvested 48 hours *post* infection (hpi).

### 2.2.3 RV production

For RV production twenty 175 cm<sup>2</sup>-cell culture flasks (353112, BD Falcon™, USA) were used to expand the 293 Flex GFP cell in the serum-supplement medium. When the cell confluence reached 80-90 % the medium was replaced by 25 mL of serum-free medium. The cell culture supernatant was collected 24 h after medium exchange.

## 2.3 Virus purification

### 2.3.1 Harvest and Clarification

After Ad5 bioreactor harvest, the cells were lysed by adding Triton X-100 (X100, SIGMA-ALDRICH®, Switzerland) to a final concentration of 0.1 % (w/w). Simultaneously, Benzonase® (101654, Merck Millipore, Germany) was added to a final concentration of 50 U/mL. The virus-containing bioreactor bulk was incubated at 37°C for 2 h.

Clarification of Ad5 bulk was performed resourcing to a Sartopore® 2 filter with 0.8 + 0.45 µm pore size (5445306G8--OO, Sartorius, Germany). Before filtration the module was primed with three capsule volumes of TRIS buffered saline, pH 8.0 (TBS; T6664, SIGMA-ALDRICH®, Switzerland). The virus-containing bulk was loaded to the filter at a constant flow rate equivalent to 150 LMH using a Tandem 1082 Pump (Sartorius Stedim Biotech, Germany).

Cell lysis and nuclease incubation was not performed for the RV-containing bulk since the these enveloped virus were collected in the cell culture medium. The RV-containing supernatant was clarified using a 0.45 µm vacuum-driven filter (SCHVU05RE, Merck Millipore, Germany). The filter was conditioned with 500 mL of TBS, pH 8.0 before virus microfiltration.

## 2.4 Body feed filtration

For the screening four filter aids were tested:

Celpure® C300 (Advanced Mineral™, USA)

Celpure® C1000 (Advanced Mineral™, USA)

Celite® (World Maetrial, USA)

Divergan® RS (BASF, Germany)

All the filter aids were kindly provided by Dr. Franziska Jonas (Downstream Process Technologies, Sartorius Stedim Biotech, Germany)

The screening procedure consisted in incubating 10 g of each of the filter aids with 50 mL of Ad5-containing lysed cell bulk at pH 4.5 and pH 7.0 (the bulk used was not treated with Benzonase® nor clarified in any way). Before adding the lysed cell bulk to the glass beakers with the filter aids a sample was retrieved, the was measured (MM40+, CRISON, Spain) and the turbidity was determined (2100Qis Portable Turbidometer, HACH®, Germany). The

mixtures were incubated at 20-22°C under constant and gentle stirring. After 30 min and 60 min of incubation the stirring was stopped (allowing the filter aid to settle by gravity) a sample was collected.

Upon sample analysis the TP and IP recovery yield ( $Y_{TP}$  and  $Y_{IP}$ ) were determined accordingly with equation 2.1 and 2.2, respectively.

$$Y_{VP} = \frac{C_{VP}V}{C_{VP,i}V_i} \quad (2.1)$$

$$Y_{IP} = \frac{C_{IP}V}{C_{IP,i}V_i} \quad (2.2)$$

Impurity – *i. e.*, DNA and HCP – clearance (%) were also assessed and calculated as defined by equation 2.3 and 2.4, respectively.

$$\text{DNA Clearance} = 1 - \frac{C_{DNA}V}{C_{DNA,i}V_i} \quad (2.3)$$

$$\text{HCP Clearance} = 1 - \frac{C_{HCP}V}{C_{HCP,i}V_i} \quad (2.4)$$

## 2.5 Ultrafiltration studies

The ultrafiltration devices were kindly provided by Dr. Tobias Schleuss (Membrane R&D, Sartorius Stedim Biotech, Germany). The membranes modules were set up accordingly with the manufactures' instructions. Briefly, a Tandem 1082 Pump (Sartorius Stedim Biotech, Germany) was used to feed the clarified bulk to the membrane device, the retentate was recycled to the feed container and the permeate was collected separately. The TMP (see equation 2.5) was controlled by adjusting the retentate flow rate using a flow restriction valve. Sartocon Slice 200 Filter Holder was used (#17525---01, Sartorius Stedim Biotech, Germany) for cassette devices. MasterFlex®14 tubing (MasterFlex Group, Germany) with 1.6 mm internal diameter was used. The pressure was monitored at feed inlet, retentate outlet and permeate outlet by in-line pressure transducers (080-699PSX-5, SciLog®, USA). Retentate temperature was measured with thermocouple sensor (56-4110-05 and PRT-DPM-3T/50, GE Healthcare Life Sciences, Sweden). The feed/retentate and the permeate volumes were monitored using a technical scale (TE4101, Sartorius Stedim Biotech, Germany).

$$\text{TMP} = \frac{P_f + P_r}{2} - P_p \quad (2.5)$$

Before any experiment the membranes were thoroughly rinsed with ultrapure water (Grade 1, as defined in ISO 3696) to eliminate trace preservatives. Membrane permeability was determined by the normalized water permeability corrected for 20°C ( $NWP_{20^\circ\text{C}}$ ,  $\text{LMH bar}^{-1} \equiv \text{L m}^{-2} \text{ h}^{-1} \text{ bar}^{-1}$ ). The  $NWP_{20^\circ\text{C}}$  (equation 2.6) was calculated based on pure

water permeate fluxes ( $J_p$ ) measured at five different TMP between 0.4 and 2.0 bar.

$$\text{NWP}_{20^\circ\text{C}} = \frac{K}{\eta} = \frac{J_p}{\text{TMP}} \text{TCF} \quad (2.6)$$

The NWP was corrected for 20°C using the temperature correction factor (TCF, equation 2.7) based on water dynamic viscosity ( $\eta$ )<sup>[128]</sup>.

$$\text{TCF} = \frac{\eta_{T^\circ\text{C}}}{\eta_{20^\circ\text{C}}} \quad (2.7)$$

This measurement was done before the experiment, after the experiment and after CIP.

After conditioning the UF system with diafiltration buffer (20 mM TRIS, pH 8.0, 25 mM NaCl), 450 mL of clarified feedstock containing Ad5 or RV were concentrated 10-fold and then were diafiltered five times. The UF/DF test was performed at a constant pressure of 1.2 bar and at a constant feed flow rate (cross-flow) equivalent to a linear velocity ( $v$ ) of 0.202 m s<sup>-1</sup> (see Table 2.1). For the RV ultrafiltration with Type H membrane it was not possible to achieve the TMP of 1.2 bar while maintaining a recirculation flow rate appropriated for TFF. Therefore, exceptionally in this case the performance test was run at a TMP of 0.9 bar. The linear velocity used was kept constant for all experiments in order to have the same tangential flow/force. Unless stated otherwise, the membranes used for RV were coated before UF experiment with 40 mL of 4 g L<sup>-1</sup> human serum albumin (HSA) prepared in buffer 1. The HSA was recirculated at 120 mL min<sup>-1</sup> for 10 min.

Throughout the filtration process samples of the retentate were collected and stored at -80°C for further analysis.

The permeate flux was recorded by means of gravimetric control and membrane throughput capacity –  $\tau$ , the amount of feed processed within a period of time ( $t$ ) using a given membrane area ( $A$ ) – was determined according to equation 2.8.

$$\tau = \frac{V_i}{At} \quad (2.8)$$

Also the shear rate at the wall ( $\dot{\gamma}_w$ ) under laminar flow conditions (Reynolds number,  $Re$ , < 2100 ) for HF and cassette modules were calculated as defined in equation 2.9 and 2.10<sup>[129]</sup>, respectively.

$$\dot{\gamma}_w = \frac{8v}{d} = \frac{4Q}{n\pi r^3} \quad (2.9)$$

$$\dot{\gamma}_w = \frac{6v}{h} = \frac{6Q}{wh^2} \quad (2.10)$$

The CIP procedure consisted of washing the UF system with 1 M NaOH at a flow rate of 500 mL/min and then a 60-min incubation. After this treatment the system was rinsed with ultrapure water until the outlet stream reached pH 7.

For the Ad5 runs, all procedures were conducted at 20–22°C, while for RV runs all procedures were performed at 8–14°C.

Table 2.1: Membrane characteristics and feed flow rates used.

Manufacturer	Membrane	Development stage	Filter material	Filter area (cm <sup>2</sup> )	Module design	Flow channel		Feed flow rate (mL/min)
						Dimensions (10 <sup>-3</sup> m) $w \times h$	$r, n$	
Competitor A	Type B <sup>b</sup>	R&D prototype	RC	200	Cassette	$30 \times 0.38$	NA	1.14
	Type C <sup>a</sup>							
	Type D <sup>a</sup>							
	Type E <sup>b</sup>							
Competitor A	Type # 2 <sup>c</sup>	PES	PES	200	Cassette	$30 \times 0.30$	NA	0.90
	Type # 4 <sup>c</sup>							
Competitor B	HF 3 <sup>a</sup>	R&D prototype	PES	155	Hollow fiber	NA	0.50, 18	1.41
	HF 5 <sup>b</sup>							
Competitor A	Type F <sup>d</sup>	Pilot production	mRC	200	Cassette	$30 \times 0.38$	NA	1.14
	Type H <sup>e</sup>							
Competitor C	HF 7 <sup>e</sup>	Commercial	PES	225	Hollow fiber	NA	0.50, 13	1.02
								124

RC: regenerated cellulose;

mRC: regenerated cellulose modified with a highly hydrophilic cross-linking;

PES: polyethersulfone;

NA: not applicable/not available;

<sup>a</sup>, <sup>b</sup>, <sup>c</sup>, <sup>d</sup> and <sup>e</sup>: The precise MWCO was not available. However it was disclosed the relative MWCO within a MWCO range;<sup>a</sup>, <sup>b</sup> and <sup>c</sup> were, respectively, the prototypes of low, medium and high MWCO considering a 300–1000 kDa range;<sup>d</sup> and <sup>e</sup> were, respectively, the prototypes of low and high MWCO considering a 500–750 kDa range;<sup>w</sup> and <sup>h</sup> are the cassette flow channel width and height, respectively;<sup>r</sup> and <sup>n</sup> are the hollow fiber internal radius and fibers number, respectively.

## 2.6 Membrane chromatography

Membrane sheets and 96-well membrane holder were kindly provided by Dr. Louis Villain (Membrane R&D, Sartorius Stedim Biotech, Germany). The membrane adsorbers functionalized with a quaternary amine (Q) had three ligand densities and two different surface structures, hydrogel-grafted and directly grafted (see Figure 2.1). The hydrogel-grafted mem-

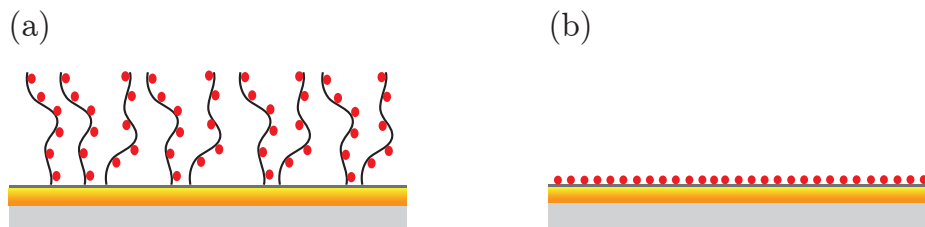


Figure 2.1: Schematic representation of the two membrane structures: (a) hydrogel-grafted membrane where the Q ligand (red dots) is immobilized in the tentacle-like structure; and (b) directly grafted membrane where the ligand is immobilized directly onto the membrane surface. Experimental design space for the hydrogel-grafted membranes.

brane had ligand densities of 1.7, 2.4 and 3.3  $\mu\text{mol cm}^{-2}$ , while the directly grafted membrane had 0.5, 2.5 and 4.5  $\mu\text{mol cm}^{-2}$ . The small-scale device had a bed volume of 23  $\mu\text{L}$  and 500  $\mu\text{L}$  of buffer or virus (clarified, concentrated and diafiltered by UF) were used. The chromatography consisted of three steps: equilibration; virus load, and elution. The equilibration buffer was 50 mM HEPES, pH 7.5 with different NaCl concentrations (0, 50, 100, 150 and 200 mM). The virus feed was diluted 1:2 with concentrated buffer to match the conductivity of the equilibration buffer. Elution was performed with 50 mM HEPES, pH 7.5, 1.0 M NaCl. After depositing the equilibration buffer inside the wells a vacuum of 0.35 bar was applied to displace the liquid across the membrane bed; the same procedure was applied for virus load and elution steps. The scale-down chromatography was performed in duplicate and the samples were stored at  $-80^{\circ}\text{C}$  until further analysis.

## 2.7 Analytical methods

### 2.7.1 Total virus particles quantification

Total virus particles concentration and size distribution were measured using the NanoSIGHT NS500 (NanoSIGHT Ltd, UK). The samples were diluted in D-PBS (14190-169, Gibco<sup>®</sup>, UK) so that virus concentration would be in the  $10^{+8}$ – $10^{+9}$  particles  $\text{mL}^{-1}$  – the instrument’s linear range. For each sample three 60-second videos were acquired and particles between 70 and 130 nm were considered.

### 2.7.2 Infectious virus particles titration

The infectious virus assay for both Ad5 and RV is based on GFP transgene expression upon infection (transfection) and flow cytometry analysis.

For Ad5 titration, 293 cells were seeded at  $0.25 \times 10^6$  cell *per* well in 24-well flat bottom plates (42475, Nunc, Denmark). After 24 h, the cells from three wells were trypsinized

and the cell concentration was determined. The cell culture medium was removed from the remaining wells and replaced with 1 mL of viral suspensions ( $10^{-1}$  -  $10^{-6}$ ) diluted in fresh medium. After 17 to 20 h, the cells were collected in Dulbecco's phosphate-buffered saline (D-PBS, 14190-169, Gibco®, UK) with 5 % FBS and immediately analyzed by flow cytometry (CyFlow®space, Partec GmbH, Germany) with GFP filters.

For RV titration, 293 T cells were seeded at  $0.20 \times 10^6$  cell *per* well in 24-well flat bottom plates (42475, Nunc, Denmark). After 24 h, the cells from three wells were trypsinized and the cell concentration was determined. The cell culture medium was removed from the remaining wells and replaced with 200  $\mu$ L of viral suspensions diluted (1/3–1/81) in fresh medium supplemented with 8  $\mu$ g mL<sup>-1</sup> of polybrene (H9268, SIGMA-ALDRICH®, Switzerland). The virus-containing medium was removed 4 h after infection and replaced with 800  $\mu$ L of fresh medium.

### 2.7.3 DNA quantification

Total DNA was quantified using the fluorescence-based Quant-iT™ PicoGreen® assay kit (P7589, Invitrogen™, UK) according to manufacture's protocol. In order to avoid matrix interference, the samples were diluted between 2–256-fold with the provided reaction buffer. The assay took place in a white 96-well microplate (437842, Nunc, Denmark) and the fluorescence was measured on a Modulus™ Microplate Multimode Reader (Turner BioSystems, now Promega, USA).

### 2.7.4 Protein analysis

Total protein was quantified using the BCA Protein Assay Kit (23225, Thermo Fisher Scientific, USA) according with the manufacture's protocol. Bovine serum albumin (BSA) was used for the calibration curve. In order to avoid matrix interference, the samples were diluted between 2- to 256-fold. The assay took place in a clear 96-well microplate (82.1581, Sarstedt, Germany) and the absorbance was measured on a SpectraMax 340PC<sup>384</sup> Absorbance Microplate Reader (Molecular Devices, USA).

Host cell protein was performed using the HEK 293 HCP ELISA Kit (F650, Cygnus Technologies, USA) following the manufacture's protocol. The standard curve was done using the 293 HCP standards provided. 1/1 000, 1/5 000 and 1/10 000 in order to allow interpolation. As suggested by the manufacturer the corrected absorbance (Abs) was used (absorbance at 450 nm minus absorbance at 650 nm).

All analytical assays performed were done in triplicate.

The protein profile was analyzed by sodium dodecyl sulphate polyacrylamide gel electrophoresis (SDS-PAGE). Pre-casted gels NuPAGE® 4-12% Bis-Tris (NP0321PK2, Novex®, UK) were used. The samples were prepared by protein precipitation and resuspension in loading mix (prepared accordingly to the manufacture's instructions) . The samples were precipitated by adding a known amount of protein to an *eppendorf* containing 1 mL of absolute ethanol (4146052, Carlo Erba Reagents, Italy). After the protein precipitation overnight at -20°C the samples were centrifuged at 13 000 *g* for 15 min and the supernatant was removed. The pellet samples were further dried by incubation at 37°C and then resuspended in the



loading mix. As molecular weight marker (MWM) 7  $\mu$ L of SeaBlue Plus2 Pre-Stained Standard (LC5925, Novex<sup>®</sup>, UK) were loaded. The electrophoresis was performed at constant voltage of 200 V for 35 min. The gel was stained with InstaBLUE<sup>™</sup> (ISB1LUK, Expedeon, UK) for 45 min under gently agitation and excess dye washed with ultrapure water. Digital image was acquired with the ChemiDoc<sup>™</sup> XRS+ (BIO-RAD, USA).



## Part III

# RESULTS AND DISCUSSION





# Body Feed Filtration

The lysed bulk turbidity was determined to be  $68 \pm 3$  NTU (average  $\pm$  standard error of the mean (SEM)) while wet cell weight (WCW) was  $8 \pm 1$  g L<sup>-1</sup>. The results presented below are corrected in order to take into account a concentration factor since it was noticed that the incubation volume – after adding the filter aid material – was reduced by 2–3-fold due to material hydration (see Figure A1, in Appendix). The Figure A2 shows the wet filter aid with 50 mL of virus bulk after settling for 48 h; up to 70 % of liquid height is filled by the filter aid material. This volumetric concentration is further supported by the analytical assays' results with virus recovery yields above 150 % and 2–3 times more DNA and HCP mass comparing with the feed bulk (when 50 mL final volumes was considered). This concentration event was also confirmed with the total protein quantification assay (data not shown). The specific concentration factor was defined considering the filter aid and liquid supernatant height.

## 3.1 Virus recovery

The incubation assays at pH 4.5 resulted in TP recoveries bellow 2 % for the Celpure C300, Celpure C1000 and Celite S filter aids. Moreover, the Celite S material also resulted in less than 2 % recovery at pH 7.0. The filter aid/pH conditions with less than 2 % TP recovery were readily excluded while the remaining were further analyzed.

The Divergan RS filter aid shown the highest TP recoveries (Figure 3.1) among the materials tested – approximately 40 % for the pH 7.0 condition. On the contrary, the Celite S resulted in the worst performance regardless of incubation time or pH-value. Both Celpure filter aids yielded TP recoveries ranging from 18 to 25 % at neutral pH. No differences were found in product recovery with increasing incubation time, except for the Divergan RS at

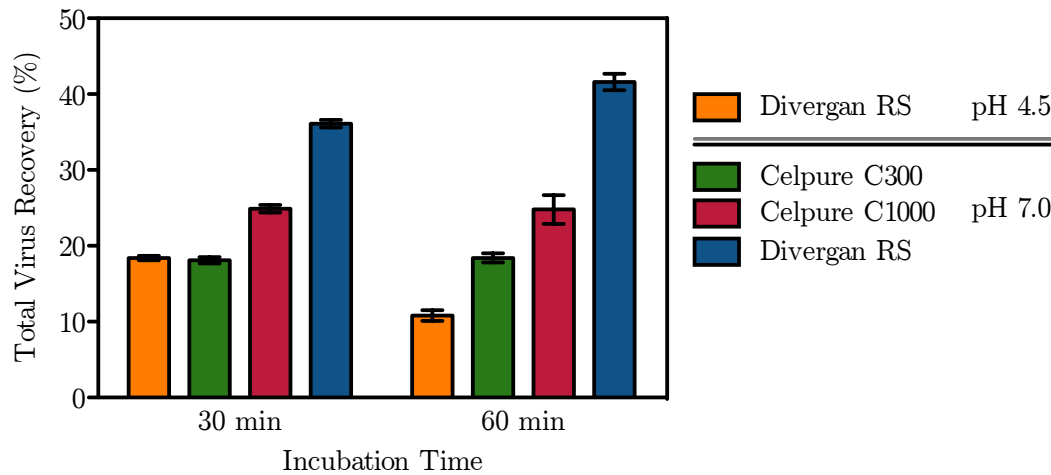


Figure 3.1: TP recovery (average $\pm$ SEM) after incubation during 30/60 minutes for the different filter aids and pH conditions.

pH 4.5. Despite a decrease in Ad5 recovery was observed in this condition, careful interpretation of this result is needed. As the pI of the Ad5 is approximately pH 4.5<sup>[36]</sup> virus aggregation and precipitation must be considered at this pH.

The IP data (Figure 3.2) confirmed the Divergan RS as the filter aid enabling the highest virus recovery. The Divergan RS material at pH 7.0 resulted in 39 % IP recovery after 30-min

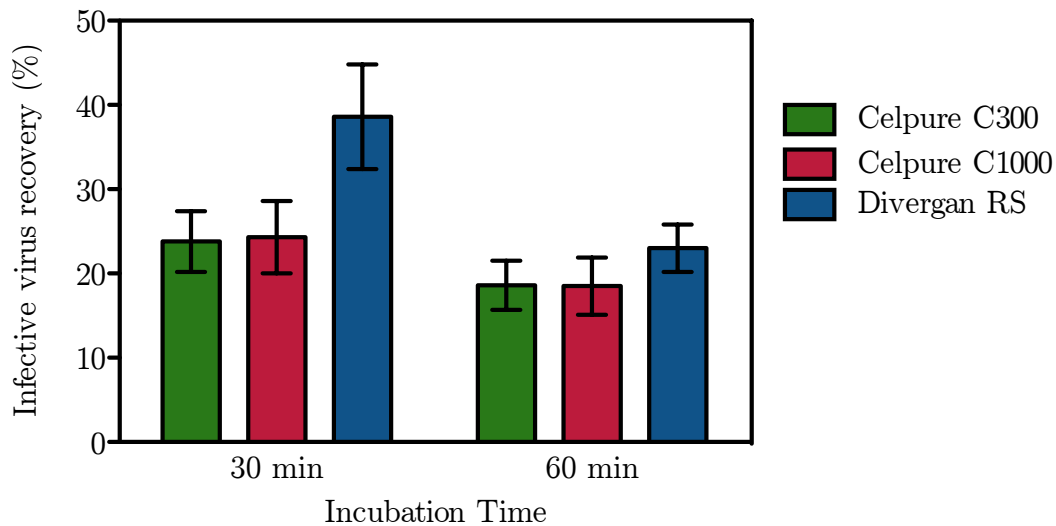


Figure 3.2: IP recovery (average $\pm$ SEM) after incubation during 30/60 minutes for the different filter aids and pH 7.0.

incubation while the Celpure C300 and C1000 recovered less than 25 % of the infective virus. Contrarily to the TP data, there is a slight decrease in IP recovery with increasing incubation time. Although Ad5 is considered a quite stable model virus<sup>[130,131]</sup>, the mechanical stress caused by mixing the filter aid micrometric particles for such a long period of time may be the explanation for the results obtained. Especially, when considering the Ad structure where the protuberant fiber protein – essential for cell adhesion and infection – is exposed more

than 10 nm out of virus capsid<sup>[32]</sup>.

## 3.2 Impurity removal

Concerning the DNA clearance (Figure 3.3), the incubation at neutral pH yielded lower DNA clearance – between 15 and 54 % – comparing with the incubation at pH 4.5, which enabled considerably higher DNA removal, close to 100 %. The enhanced DNA clearance at pH 4.5 might be due to low pH-induced precipitation and aggregation with the virus particles<sup>[72]</sup>. Celpure C300 showed the best DNA removal capacity at pH 7.0. Although

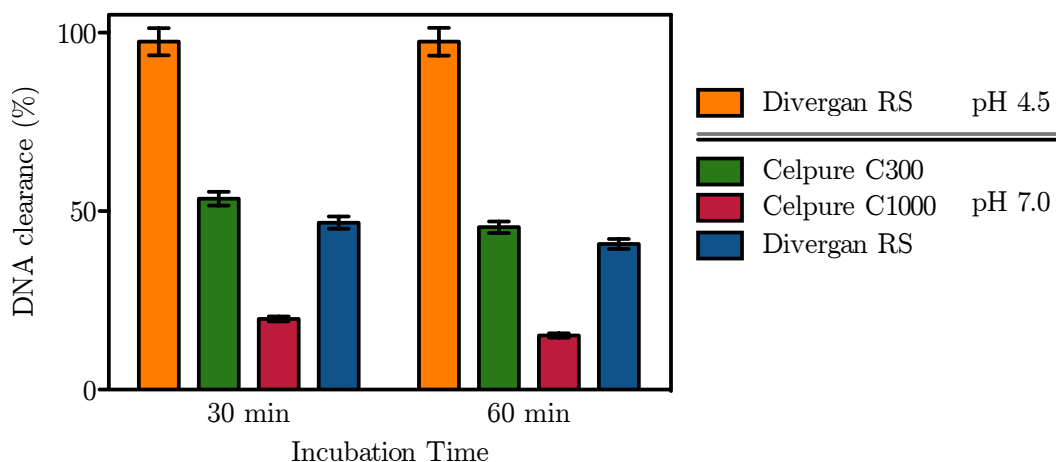


Figure 3.3: DNA clearance (average $\pm$ SEM) after incubation during 30/60 minutes for the different filter aids and pH conditions.

this DE is a negatively charged material<sup>[132]</sup>, other types of interactions – like entrapment, flocculation or hydrophobic interaction – might be responsible for the high DNA clearance. A similar phenomenon was observed recently in cation exchange (CEX) chromatography<sup>[133]</sup>. The publication reports the binding of DNA present in a post-Protein A mAb pool under low conductivity (5 mS cm<sup>-1</sup>) and its elution upon a conductivity increase to 70 mS cm<sup>-1</sup>. The Celpure C1000 is also negatively charged, however resulted in lower DNA clearance which can be explained by the smaller specific area, up to 75 % less of the specific area of Celpure C300 material<sup>[132]</sup>. Contrarily, the Divergan RS filter aid is not charged, even so it led to DNA removal rates close to those of Celpure C300. The Divergan RS has a specific area of  $\sim 55 \text{ m}^2 \text{ g}^{-1}$  (estimated based on filter aid density and an average diameter of 90  $\mu\text{m}$ <sup>[134]</sup>), which is one order of magnitude higher as compared with the Celpure C300. Besides the different – non-electrostatic – interaction mechanism, the high specific area of Divergan RS might contribute also for the high DNA clearance.

Considering the HCP clearance (Figure 3.4), the results ranged from 50 to 80 %. Since HCP is a complex array of proteins with different molecular size, charge, pI and stability, the incubation at acidic pH did not provide substantial HCP clearance, contrary to what was observed for DNA. Perhaps this is also why no remarkable difference was observed between both Celpure's DE and the synthetic Divergan RS. Additionally, incubation for a long period of time did not increase neither HCP nor DNA removal.

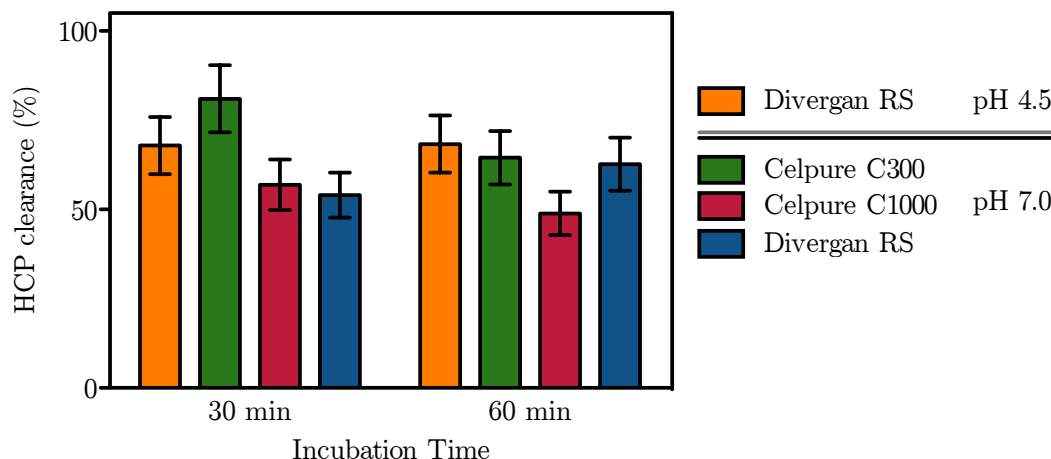


Figure 3.4: HCP clearance (average $\pm$ SEM) after incubation during 30/60 minutes for the different filter aids and pH conditions.

### 3.3 Discussion

The Celite S material was readily excluded as no virus particles were recovered regardless of incubation time or pH-value. On the contrary, the two other DE-based filter aids enabled virus recoveries between 18 and 25 % when used at pH 7.0. The major difference between the Celite S and the Celpure materials lies in the SiO<sub>2</sub> purity and metallic oxides content<sup>[132]</sup>. The Celite S material is a material less pure with a greater metal content when compared with the Celpure DE. The DE purity seems to limit virus recovery and should be considered when developing purification strategies such as the BFF.

Low virus recoveries were observed when the incubation was performed at pH 4.5, as expected since the virus has a acidic pI. However, the results obtained show that the non-charged material might be employed at acidic pH. This could be an advantage if a vaccination application (which does not require infective virus) is envisioned, nevertheless pH and conductivity should be further optimized for TP recovery and impurity removal.

The synthetic material Divergan RS resulted in the highest TP and IP recoveries while maintaining HCP and DNA removal capacities comparable with the charged Celpure C300. Even so the Divergan RS allowed for less than 50 % of product recovery. The low yields can be explained by the small-scale set-up and protocol used. The experiment was focused on filter aid screening therefore the Ad5 bulk was overloaded with DE to a final concentration of 200 g L<sup>-1</sup> – approximately 10-fold higher than those to be used in a scalable filtration trial. While overloading is suitable for a initial material selection, it might lead to lower virus recovery.



# Ultrafiltration

## 4.1 R&D prototypes

### 4.1.1 Hydraulic permeability

All eight UF prototypes were characterized and the  $NWP_{20^{\circ}C}$  is reported in Figure 4.1. The two PES cassettes registered the highest  $NWP_{20^{\circ}C}$ , up to  $924 \text{ LMH bar}^{-1}$ , which may

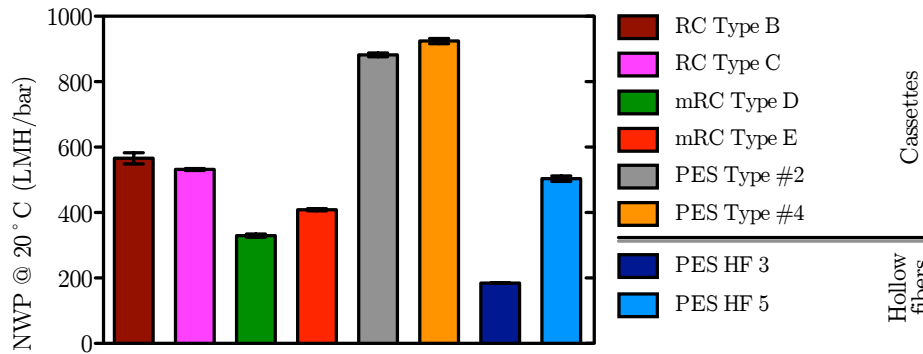


Figure 4.1:  $NWP_{20^{\circ}C}$  (average  $\pm$  standard error of the mean (SEM)) for the different R&D UF prototypes provided.

be explained due to the high MWCO. Both RC cassettes exhibited  $NWP_{20^{\circ}C}$  close to  $560 \text{ LMH bar}^{-1}$  whereas the mRC permeability only reached  $400 \text{ LMH bar}^{-1}$ , probably due to different construction material and/or manufacture (*e. g.* flow channel height). Regarding the HF, these modules shown lower permeability when compared with the PES cassettes and some of the RC-based cassettes. As expected the lower MWCO displayed lower permeability than the HF of higher MWCO, since their features are identical (number of fibers *per* module,

fibers' internal diameter and membrane material).

#### 4.1.2 Virus recovery

Samples were collected during the UF when 3, 5 and 10 concentration factors (CF) were achieved and also after 2 and 5 diafiltrations (DF). The samples were further analyzed to determine the filtration performance of each UF device. The Figure 4.2 and Table 4.1 show the TP and IP recovery, respectively.

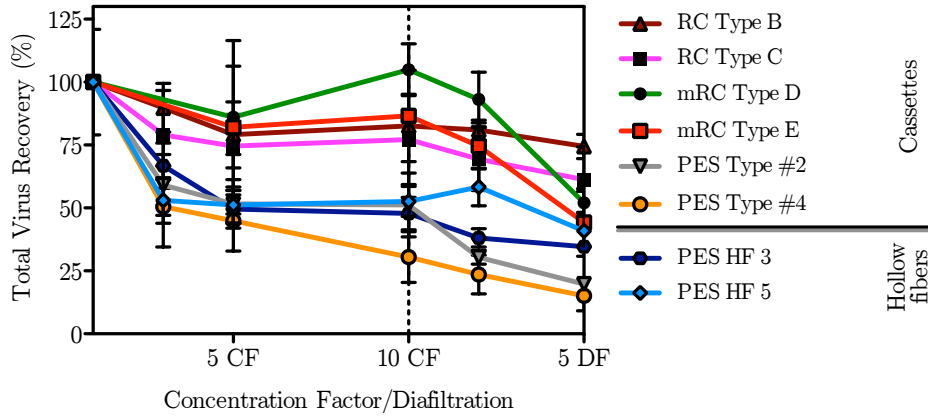


Figure 4.2: Total virus particles recovery (average $\pm$ SEM) as function of concentration factor/diafiltration volume for the different R&D UF prototypes.

All RC-based cassettes were capable of the high TP recoveries, ranging from 69 up to 93 % after 2 DF. Contrarily, the PES-based membranes allowed for virus permeation as shown by the low TP recovery (23–58 %). In part this was expected, since the PES cassettes have the highest MWCO.

The IP data presented in Table 4.1 is in agreement with the TP recovery. All the RC-

Table 4.1: IP recovery and processing time for 10-fold concentration for the different R&D UF prototypes.

Module	Material	Prototype	IP recovery (% $\pm$ SEM)	Processing time (min)	Shear rate (s <sup>-1</sup> )
Cassette	RC	Type B	94 $\pm$ 14	14	3186
		Type C	85 $\pm$ 11	30	
	mRC	Type D	79 $\pm$ 11	24	
		Type E	103 $\pm$ 13	14	
	PES	Type #2	89 $\pm$ 16	19	4037
		Type #4	54 $\pm$ 11	17	
Hollow fiber	PES	HF 3	60 $\pm$ 4	105	1613
		HF 5	8 $\pm$ 2	48	

based cassettes were able to recover between 79 and 100 % of infective virus particles at the end of the concentration step. Interestingly, between these four modules, the ones with larger MWCO were the ones with higher IP recoveries, close to 100 %. This result points towards the importance of optimizing the choice of cassette and MWCO for the lowest processing time to avoid loss of infectivity due to shear-induced damage.

Following the same trend observed in TP recovery, the Type #2 cassette allowed for a higher IP recovery as compared with the PES #4 module. These PES cassettes have the same membrane material and the same MWCO; however, slight differences, such as a broader (or narrower) pore size distribution, could impact the prototype's virus recovery<sup>[84]</sup>.

The HF prototypes had low recovery of IP. This can be explained by the longer processing times. For instance, the HF 3 module took seven times longer than the Type B or Type E prototypes to perform the same 10-fold concentration. Even so, the HF 3 showed a moderate IP recovery ( $60 \pm 4$  %).

### 4.1.3 Impurity removal

#### 4.1.3.1 Protein clearance

The HCP analysis presented in Figure 4.3 shows that both PES cassettes were able to remove 86–91 % of the HCP present, as expected due to high MWCO. The remaining

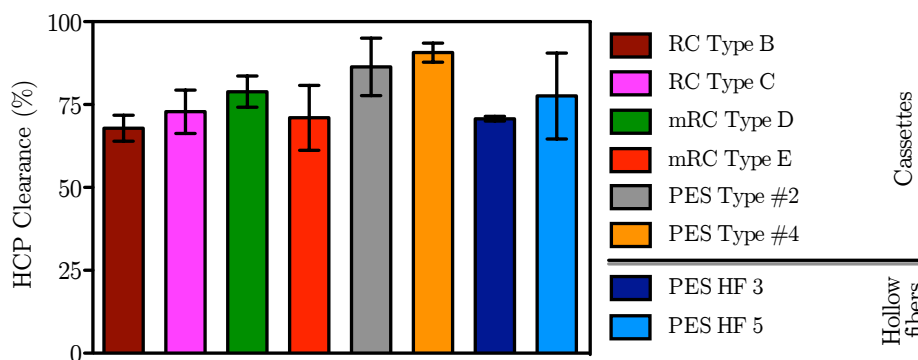


Figure 4.3: HCP clearance (average  $\pm$  SEM) after 2 diafiltrations for the different R&D UF prototypes.

prototypes were able to remove between 70 and 80 % of HCP, in agreement with the literature of UF step<sup>[72,95]</sup>.

All four RC-based UF membranes show a marked enrichment in Ad5 protein bands as compared with the feed in the SDS-PAGE (Figure 4.4), in agreement with the high TP and IP recovery yields. This is specially visible with the virus' major capsid protein (hexon, 109 kDa) and resulted from the successful volumetric concentration and virus retention. Also, the PES hollow fibers led enrichment in hexon protein, however not as much as the RC-based modules. Furthermore, as demonstrated by TP recovery, the PES cassettes tend to retain less virus due to their high MWCO.

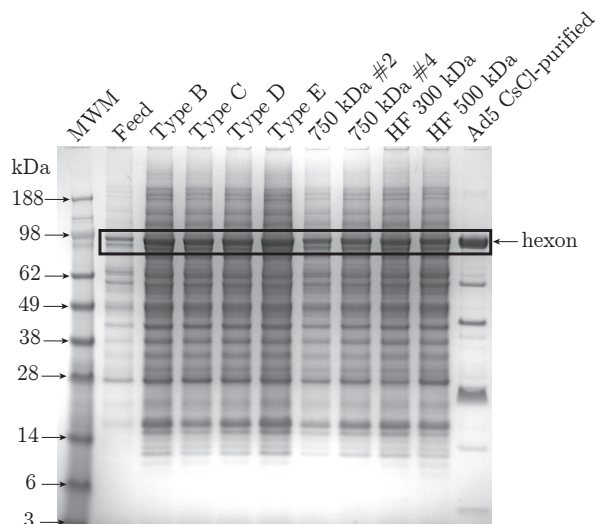


Figure 4.4: Total protein profile analyzed by SDS-PAGE after 2 DF in comparison with the feed and a CsCl ultracentrifugation-purified Ad5 standard. Each well was loaded with 15  $\mu$ g of total protein.

#### 4.1.3.2 DNA clearance

Both PES-based cassettes enabled higher DNA clearance – 85% – than the remaining prototypes (Figure 4.5). The Type B, Type C, Type D, Type E and HF 5 prototypes shown

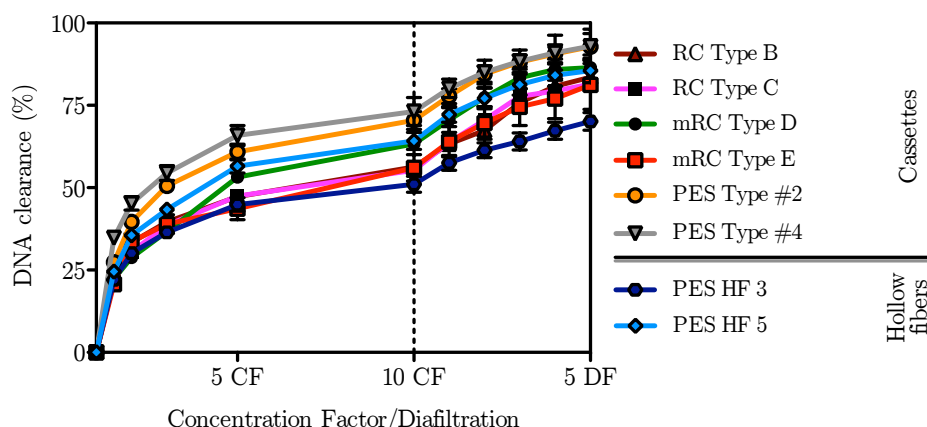


Figure 4.5: DNA clearance (average $\pm$ SEM) as function of concentration factor/diafiltration volume for the different R&D UF prototypes.

intermediate DNA clearances (67–70%) and the HF 3 shown the worst DNA clearance (61 %). Both the HCP and DNA clearance data are in agreement and point out both PES cassettes as the best modules regarding impurity removal. However, considering also TP and IP data, these modules were not as efficient as the RC-based membranes.

#### 4.1.4 Productivity analysis

The permeate flux over time and throughput (feed processed *per* membrane area and time,  $\text{L m}^{-2} \text{h}^{-1}$ ) were also evaluated for all UF prototypes studied (Figure 4.6).

The Figure 4.6(a) shows that all membranes except Type D were able to maintain an essentially stable flux, due to the TMP-constant operation. On the other hand the Type D

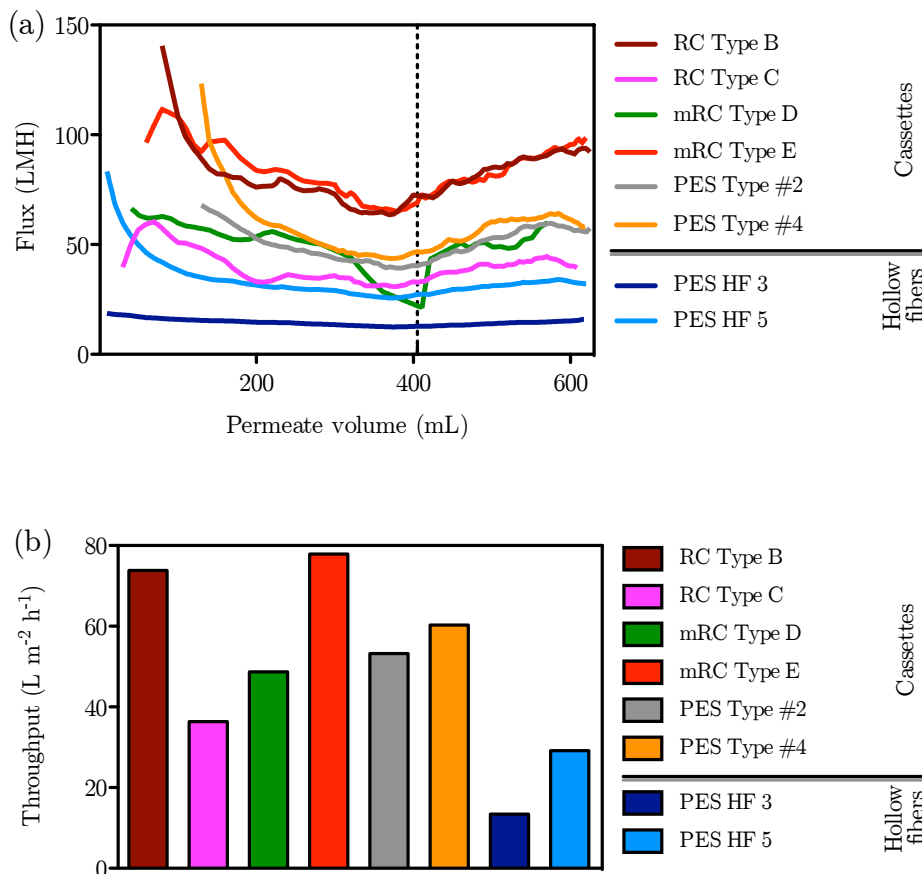


Figure 4.6: (a) Permeate flux throughout filtration and (b) throughput capacity for each R&D UF prototype assayed (considering a 10-fold concentration and 2 DF).

shown a marked flux decrease between 300 to 405 mL of permeate volume (between 3 to 10 CF). However, complete fouling was not observed. It is also important to point out that the two UF modules which displayed superior throughput (Figure 4.6(b)) – RC Type B and mRC Type E – were also the ones showing highest virus recoveries. This combination makes them modules of high productivity (product recovered *per* membrane area and time).

#### 4.1.5 Flux Recovery

The after-use flux recovery enables assessment of the degree of irreversible/strongly associated foulants accumulated on the membrane during filtration. On the other hand, the after-CIP flux recovery permits to evaluate the loss of permeability after a complete cycle. This metric is an industrial relevant indicator as it serves as benchmark of membrane performance, is used to assess performance decay and also cleaning-in-place (CIP) protocol effectiveness. The flux recoveries (flux over initial flux,  $J/J_0$  (-)) are presented in Figure 4.7.

Three membranes (Type B, Type D and Type E) have shown a reduced fouling compared to the others. These results can be related, in part, with different hydrophilic properties of the membranes' material. In contrast, RC Type C was not able to recover to its initial flux to the same extent as the Type B, possibly due to the lower MWCO. All PES-based prototypes had low after-use flux recovery. Considering the wide range of MWCO of these

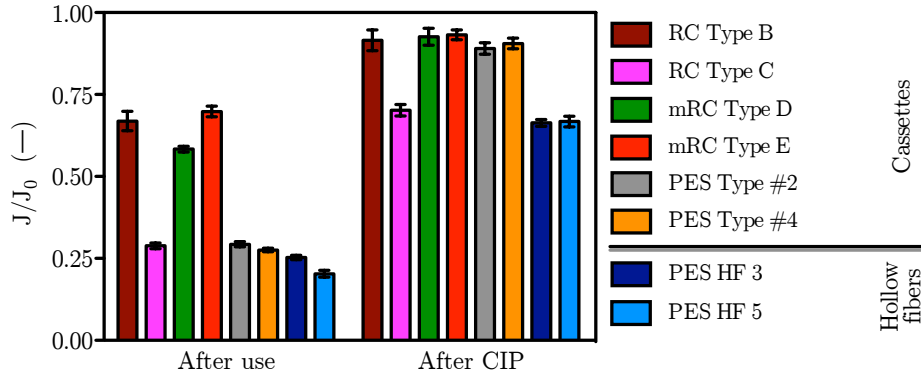


Figure 4.7: Flux recovery (average $\pm$ SEM) after-use and after-CIP for the different R&D UF prototypes

prototypes, the results suggest that PES UF membranes might be more prone to adsorbing biomolecules<sup>[74,90]</sup>.

Regarding the after-CIP flux recovery, it was clear that the PES cassettes, the Type B and both mRC cassettes regained their permeability (with flux losses ranging between 7 and 11%). Meaning that these UF modules withstood a complete cycle and might be used as a repeated-use device; although the number of cycles allowed was not assessed. The remaining modules (RC Type C and both PES hollow fibers) shown loss of water permeability after one cycle, and might not be suited for repeated-use device.

## 4.2 Commercial/pilot production devices

The results obtained with R&D UF prototypes were used to adjust the membrane features. A new set of improved UF membranes produced by a fully scalable manufacturing line was evaluated for Ad5 and RV ultrafiltration.

### 4.2.1 Hydraulic permeability

The mRC Type H cassette displayed the highest  $NWP_{20^\circ C}$  – 889 LMH bar<sup>-1</sup>, Figure 4.8 – possibly due to the high MWCO. As expected the Type F cassette shown lower  $NWP_{20^\circ C}$

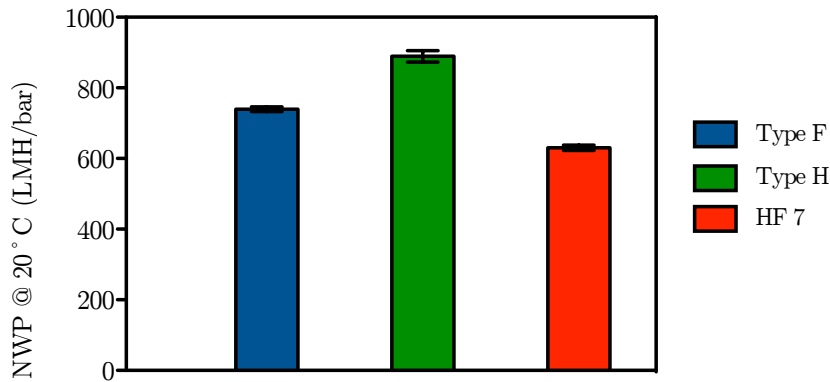


Figure 4.8:  $NWP_{20^\circ C}$  (average $\pm$ SEM) for the different UF devices studied.

– 739 LMH bar<sup>-1</sup>. The  $NWP_{20^\circ C}$  for the HF 7 was determined to be 630 LMH/bar. The

lower permeability of the HF 7 comparing with the same cut-off cassette might be explained by differences in membrane material and/or module design.

#### 4.2.2 Virus recovery

Samples were collected during the UF when 3, 5 and 10 concentration factors (CF) were achieved and also after 2 and 5 diafiltrations (DF). The samples were further analyzed to determine the filtration performance of each UF device.

The Ad5 experiments resulted in TP recoveries ranging from 50 % (Type H) up to 75 % (Type F) after 10-fold concentration (Figure 4.9); however two diafiltration (DF) volumes decreased the recovery yield to 40 % for all membranes assayed.

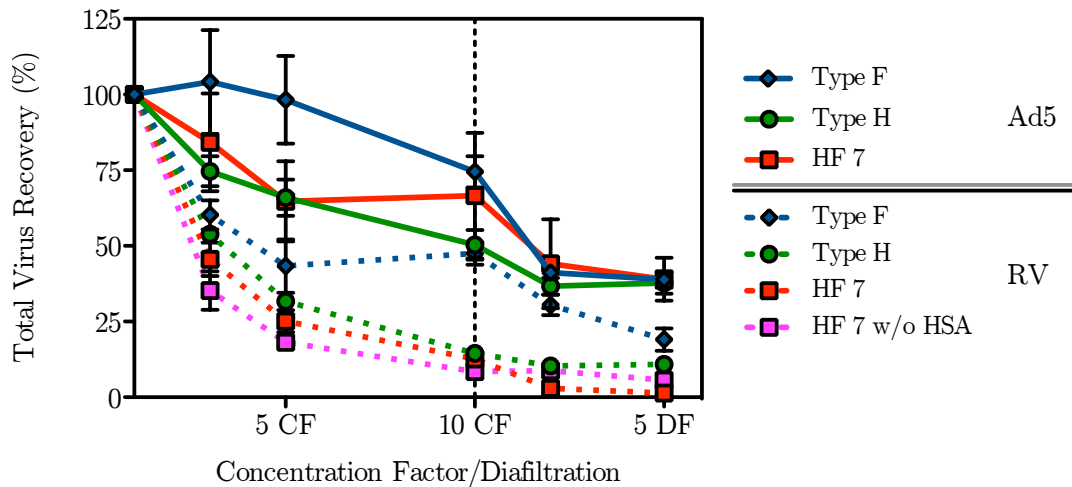


Figure 4.9: Total virus particles recovery (average $\pm$ SEM) as function of concentration factor/diafiltration volume for the different UF devices.

The RV experiments yielded lower recoveries for all UF devices; Type F (lower MWCO) membrane had the higher TP recovery of 48 %. The remaining membranes were only able to recover between 8 and 14 % of RV particles. It has been suggested that coating membrane filters with HSA leads to lower RV losses<sup>[83,93]</sup>, however in this case the HSA coating did not increase RV recovery when the PS HF was tested.

The IP data (Table 4.2) shows the same trends observed in TP recovery for both Ad5

and RV.

Table 4.2: IP recovery and processing time for 10-fold concentration for the different UF devices.

Virus	Module	Material	Device	IP recovery (%±SEM)	Processing time (min)	Shear rate (s <sup>-1</sup> )
Ad5	Cassette	mRC	Type F	124.9±12	17.5	3186
			Type H	93.6±16	17.2	
	Hollow Fiber	PS	HF 7	111.7±13	26.4	1619
RV	Cassette	mRC	Type F	8.9±1	4.4	3186
			Type H	13.5±3	3.8	
	Hollow Fiber	PS	HF 7	15.3±3	3.3	1619
			HF 7 †	15.9±1	3.8	

†The UF membrane was not coated with HSA (see Section 2.5, page 20).

The Type F and HF 7 membranes were able to fully recover the infective Ad5 while Type H membrane achieved 94 % recovery. As observed for TP recovery, Type H resulted in the lowest recovery, possibly due to its high MWCO. Despite being rated with the same MWCO as the Type H cassette, the HF 7 was able to recover more infective Ad5, which could be explained by the lower shear rates associated with its operation.

As observed previously, the low RV recoveries were also confirmed by the low IP recoveries, between 9 and 16 %. The only exception was the Type F membrane whose discrepancy between TP and IP data suggests that virus functionality was lost, possibly due to shear-induced damage.

### 4.2.3 Impurity removal

#### 4.2.3.1 Protein clearance

The mRC Type F and Type H cassettes removed 67 and 68 % of HCP, respectively, while the PS-based HF 7 was able to achieve 86 % HCP clearance (Figure 4.10). The higher HCP

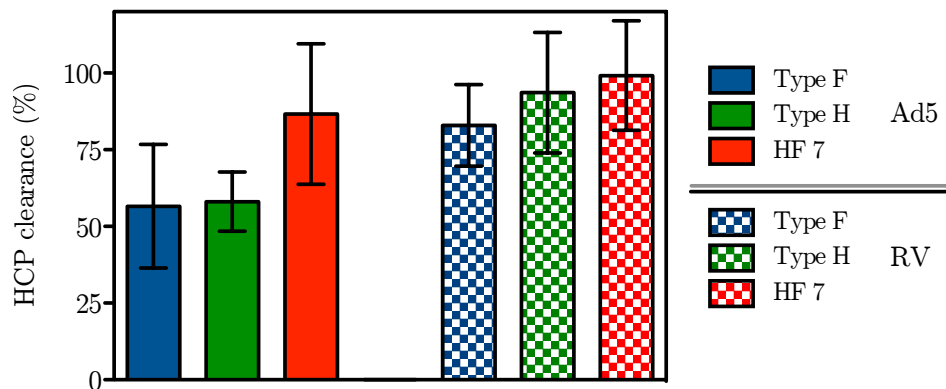


Figure 4.10: HCP clearance (average±SEM) after 2 diafiltrations for the different UF devices.

protein clearance registered for the HF might be due to the different filter material, which is more hydrophobic than RC, and thus more prone to adsorption. The protein clearance



obtained is in agreement with the available data for the UF step<sup>[72,95]</sup>.

For the RV runs the HCP clearance was higher compared with those obtained for Ad5; in this case 83, 94 and 99 % HCP was obtained for Type F, Type H and HF 7, respectively. These values are slightly higher comparing with has been reported for RV UF<sup>[83,135]</sup>, with protein clearance rates in the 70–80 % range. The higher protein clearances for the RV runs were expected since no cell lysis step was performed and thus the RV feed contains essentially small proteins present at low concentrations in cell culture supernatant.

The protein profile (Figure 4.11) regarding the Ad5 experiments shows a clear enrichment in Ad5 proteins' compared with the feed, which is in agreement with the high virus recoveries registered. The volumetric concentration is particularly evident on the adenovirus' major capsid protein band (Hexon, 109 kDa). With the RV UF it is also possible to observe

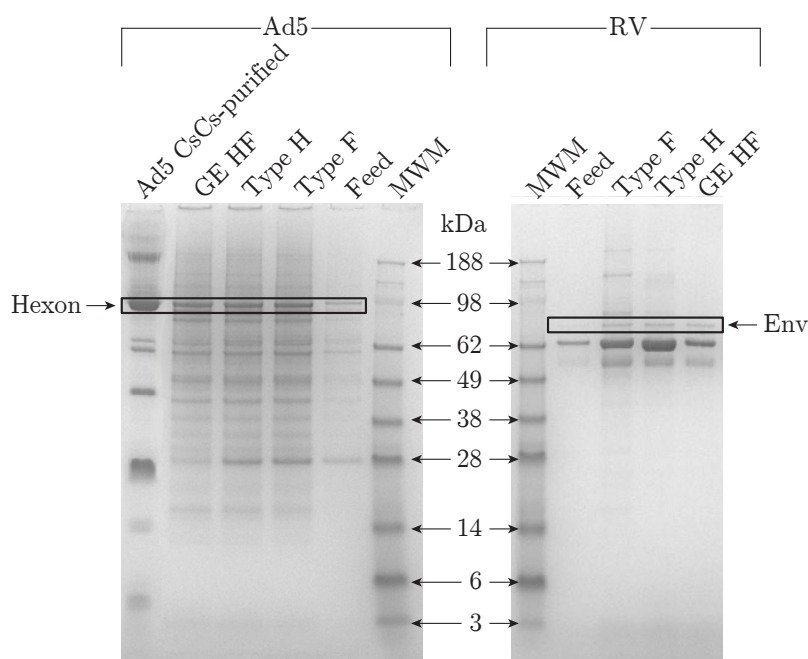


Figure 4.11: Total protein profile analyzed by SDS-PAGE after 2 diafiltration volumes in comparison with the feed. The left gel concerns the Ad5 runs and a CsCl ultracentrifugation-purified Ad5 standard, whereas the right gel corresponds to the RV experiments. Each well was loaded with 15  $\mu$ g of total protein.

the concentration and retention of retroviral particles, particularly on the virus' envelop glycoprotein (Env, 70 kDa) which is enriched comparing with the feed. The slight enrichment is in accordance with the low recoveries obtained; however it is not possible to distinguish between the different membranes.

#### 4.2.3.2 DNA clearance

The DNA analysis performed (Figure 4.12) revealed that lower DNA removal was achieved in Ad5 runs compared with RV experiments. One of the challenges of Adenovirus purification is host cell DNA removal since the bioprocess comprises a cell lysis step<sup>[136]</sup> but also because it has been shown that DNA can associate with the virus particle resulting in co-purification of both species<sup>[72]</sup>. For the Type F and Type H cassettes the DNA clearance after two DF

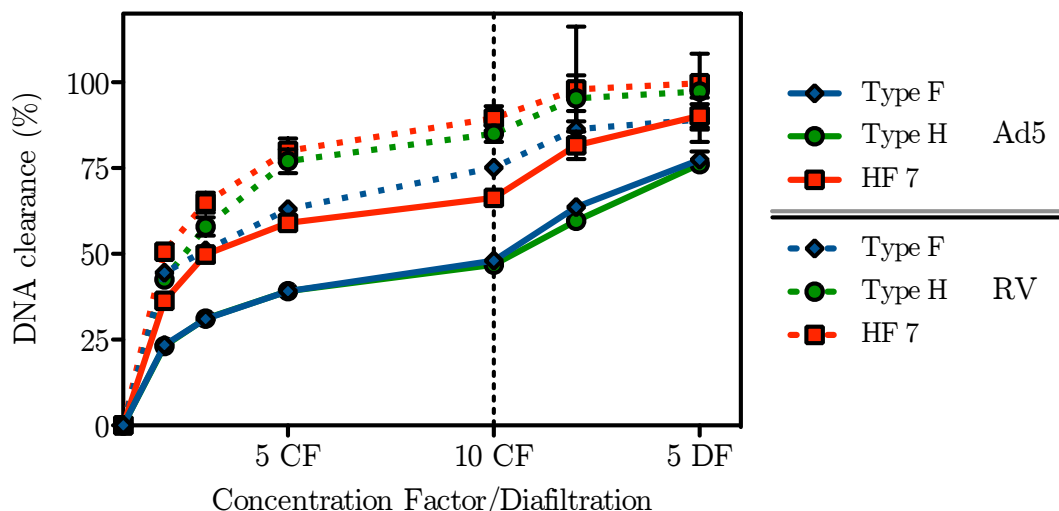


Figure 4.12: DNA clearance (average $\pm$ SEM) as function of concentration factor/diafiltration volume for the different UF devices.

was 64 and 60 %, respectively, while the HF 7 was able to remove 82 % of DNA present in the Ad5 feed. In the range of MWCO assayed, there was no observed difference between medium and high MWCO cassettes, therefore the higher HCP and DNA clearance observed with PS-based HF 7 membrane might be due to adsorption. Considering the RV experiments, the Type H and HF 7 removed 95 and 98 % of the DNA present, respectively, while the Type F membrane enabled slightly lower DNA clearance (86 %).

#### 4.2.4 Productivity analysis

As with the previous set of membranes, the permeate flux over time and throughput (feed processed *per* membrane area and time) were evaluated for all UF devices (Figure 4.13). The Figure 4.13(a) shows that all membranes were able to maintain an essentially stable flux during the TMP-constant operation, and no device shows signs of fouling. It is also important to point out that the higher permeate fluxes achieved for RV are consequence of the clearer starting material, as stated earlier.

When the UF devices were challenged with the Ad5 clarified bulk it is evident the higher throughput of the mRC-based membranes compared with the PS-based HF 7 (Figure 4.13(b)). Particularly, the Type F membrane – which combines high throughput capacity with the highest TP and IP recoveries – is a high productivity module (product recovered *per* membrane area and time). However, when the clearer RV-containing supernatant was used the advantages of module design and filter material are no longer evident. In this case throughput capacity displayed a similar trend, related to the hydraulic permeability (Figure 4.8).

#### 4.2.5 Flux Recovery

The after-use flux recovery enables assessment of the degree of irreversibly/strongly associated foulants accumulated on the membrane during filtration. The after-CIP flux recovery permits to evaluate the loss (or gain) of hydraulic permeability after a complete cycle. The

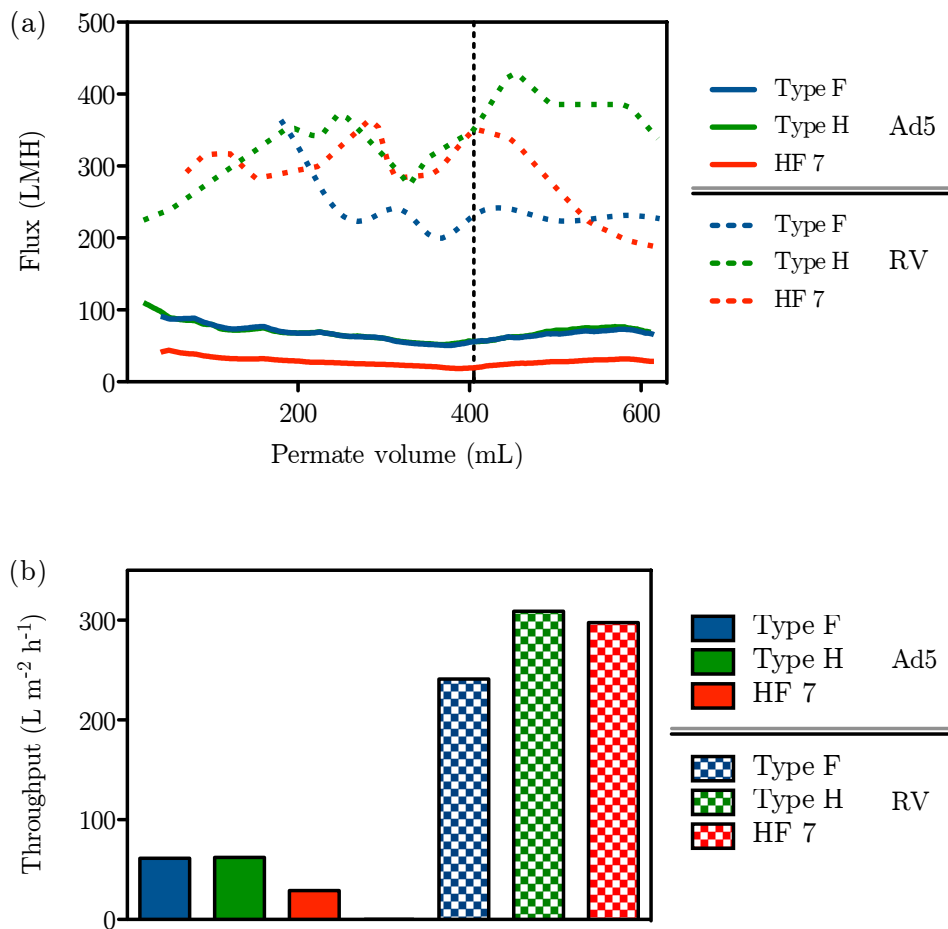


Figure 4.13: (a) Permeate flux throughout filtration and (b) throughput capacity for each UF device assayed (considering a 10-fold concentration and 2 DF).

flux recoveries ( $J/J_0$ ) are presented in Figure 4.14.

The two mRC cassettes have shown a reduced fouling compared with the PS hollow fiber (HF 7) in both Ad5 and RV trials. This fouling is particularly evident when Ad5 is used, resulting in flux recovery of 24 % for the HF 7 while the cassettes were able to recovery up to 58 % of the initial flux. The results suggest that the PS-based UF devices might be more prone to fouling through adsorption of biomolecules.

After CIP, both the mRC cassettes fully recovered their permeability (96 and 97 % flux recovery). This provides a good indication for membrane as a reusable device. Contrarily, the HF 7 shows performance decay after CIP, since its hydraulic permeability was increased by 17 % after the CIP protocol recommended by the manufacturer. A unstable membrane could then be responsible for changes in the product and/or impurities retention rate.

## 4.3 Discussion

### R&D UF prototypes

Concerning the R&D prototypes (reported in the first part of this chapter), the PES hollow fiber modules have shown the worst performance under the conditions evaluated.

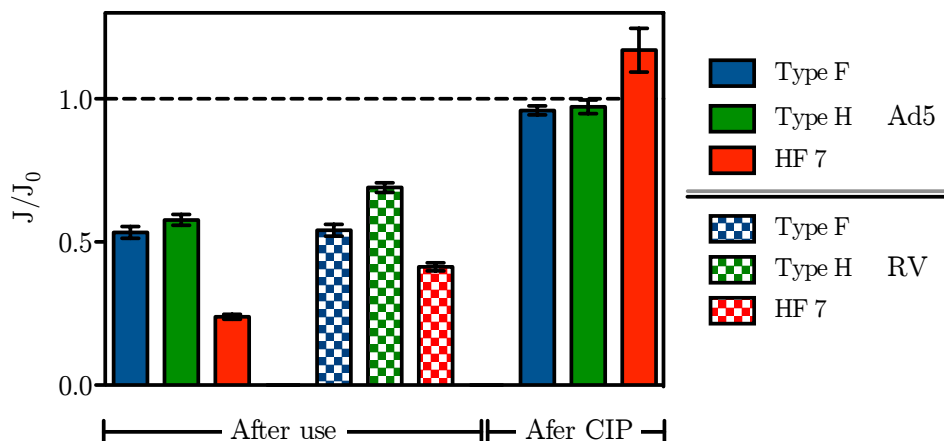


Figure 4.14: Flux recovery (average $\pm$ SEM) of the different UF devices evaluated after-use for Ad5 and RV runs and after-CIP for the Ad5 run

This is supported by the lower IP recoveries and longer processing times. While the HF 5 lost nearly all virus, the HF 3 was still able to recover 60% of IP but the long processing time is a considerable disadvantage. The results obtained by the PES R&D prototypes, namely virus recovery, are below what has been described in the literature for this MWCO range. For instance, 300 kDa HFs from GE was able to concentrate an Ad5 bulk 10-fold with 96 % IP yield<sup>[66]</sup>. In another report<sup>[97]</sup>, a 300 kDa HF (GE) and 400 kDa HF (Spectrum Laboratories) were used enabling Ad5 recoveries of 83 and 100 %, respectively.

The RC-based R&D prototypes have shown better performances, especially concerning VP and IP recovery. The Type B and Type E membranes registered similar or even better virus recovery yields than what has been reported for Ad5 ultrafiltration<sup>[66,95,97]</sup>. The RC Type B and mRC Type E have shown minimal IP loss, with IP recoveries above 94%, meaning that shear rates used are not damaging for this product. These membranes displayed similar HCP clearance (68 and 71%) and DNA clearance (67 and 70%, respectively)<sup>[72,95,135]</sup>. These two modules also possessed high throughput capacities, being able to process up to 77 L of feed within 1 hour using 1 m<sup>2</sup> ultrafiltration module. (The throughput analysis was done considering a 10-fold concentration and 2 buffer exchanges.) Considering the unit operation and early stage in downstream processing train, high recovery yields and high throughput capacities are preferred over high impurity removal rates.

### Commercial/pilot production UF devices

Considering the commercial/pilot production UF devices (presented in the last part of this chapter), the Type H membrane (high MWCO) has shown high virus recovery yield and was able to recover up to 97 % of infective Ad5, which is an improvement compared with the recovery described in the literature for a similar MWCO HF<sup>[66]</sup>. Despite the promising results with the Ad5, similar results were not achieved for the RV. Protein and DNA removal rates were close to what was observed with the other UF membranes and are in agreement with what has been reported for both Ad5 and RV ultrafiltration steps<sup>[72,95,135]</sup>.

The HF 7 was also capable of delivering high Ad5 recovery, with full IP recovery. However

as observed for the Type H cassette, the HF with the same MWCO was not capable of RV concentration, resulting in low yields. Considering impurity removals, the PS HF seems to enable slightly increased DNA and HCP clearance comparing with mRC cassettes; this was more evident with the Ad5 bulk. This increased impurity removal might be due to adsorption phenomenon rather than a size exclusion mechanism as the filter material's properties are more hydrophobic<sup>[74,90]</sup>.

The Type F cassette presented the best results among the assayed membranes. This is supported by the complete recovery of infective Ad5, an improvement comparing with what is described in the literature for 500 kDa HF<sup>[66]</sup>. Additionally, this was the only device able to partially retain and concentrate RV. Although the Type F module was able to concentrate RV, the low IP yield suggests that shear-induced damage might be compromising infective RV recovery. The results indicated that lower MWCO did not decrease impurity removal when comparing between the two mRC cassettes.

Another important feature of the Type F (and H) cassette(s) is their higher throughput comparing with the HF 7. For instance, Type F module is capable of processing up to 61 L of Ad5 clarified bulk within 1 h using a 1 m<sup>2</sup>-membrane while the GE HF can process only 29 L with the same time and membrane area (considering a 10-fold concentration and 2 DF). Although the Type F throughput is 20 % lower compared with those obtained for the best R&D prototype previously evaluated, careful comparison of such values is required since the previous membranes' MWCO might be slightly different and the manufacturing process was different.

Retrovirus purification is extremely challenging due to the labile nature of the virus particle and low titers achievable. The results achieved for Type F membrane – concentration of TP without the corresponding increase in IP titer – suggest that there is loss of virus functionality possibly due to shear-induced damage. One possible improvement would be to decrease the shear rate by lowering the feed flow rate (and consequently the TMP in order to maintain a tangential flow at the membrane's surface). The literature is scarce on purification of RV by UF<sup>[83,93,135,137]</sup>, however careful examination allows to identify two other explanation the low RV observed. First, MWCO in the 100–500 kDa range are preferred for RV concentration, as observed in this study and supported by the literature<sup>[83,135]</sup>. Second, the use of high membrane loads (feed volume *per* membrane area) might also be advantageous given the low titers characteristic of RV. The same manuscripts<sup>[83,135]</sup> report membrane loads ranging from 73 up to 133 L m<sup>-2</sup> while in our trials membrane loading was limited to 22.5 and 20 L m<sup>-2</sup> for the cassettes and HF, respectively. These three factors – shear rate, MWCO and membrane load – might explain, at least partially, the low RV recoveries achieved.

The work performed characterized in-depth several ultrafiltration membranes. The results herein presented identify UF membrane modules alternative to the currently available HF devices for virus purification. Type F (close to 500 kDa) is suggested for Ad5 concentration. This module shows complete IP recovery and impurity removal similar to those described in the literature. The key advantage of this UF module lies in the substantially shorter processing times comparing with the other membranes evaluated and described in the literature. Considering the RV, several improvement strategies were suggested based on successful RV

UF reports available in the literature.



# Membrane chromatography

*adapted from:*

Nestola, P., Villain, L., Peixoto, C., Martins, D.L., Alves, P.M., Carrondo, M.J.T., Mota, J.P.. Impact of grafting on the design of new membrane adsorbers for virus purification. *Biotechnol Bioeng*, submitted.

---

The membrane adsorbers functionalized with a quaternary amine (Q) had three ligand densities and two different surface structures (hydrogel-grafted and directly grafted). A 96-well chromatographic system was used to evaluate the impact of these features on the membrane performance.

## 5.1 Hydrogel-grafted membranes

### 5.1.1 Virus recovery

Analysis of the flow-through detected less than 5 % of the loaded virus which is in agreement with other reports where adenovirus are generally purified in bind/elute mode using Q-AEX chromatography with hydrogel-grafted membranes<sup>[67,80]</sup>.

Considering the virus recovery after elution with 1 M NaCl, the data displayed in Figure 5.1 show that low conductivity during loading results in recovery yields below 50 % regardless of the ligand density. The high ligand density adsorber ( $3.3 \mu\text{mol cm}^{-2}$ ) resulted in the lowest virus recoveries, as observed previously with Baculovirus<sup>[119]</sup>. The use of medium ligand density membrane ( $2.4 \mu\text{mol cm}^{-2}$ ) resulted in the highest recovery yields ranging from 50 % to 80 %. These recovery yields are in agreement with what was published for chromatographic purification of Ad5 using Sartobind Q<sup>[66]</sup>.

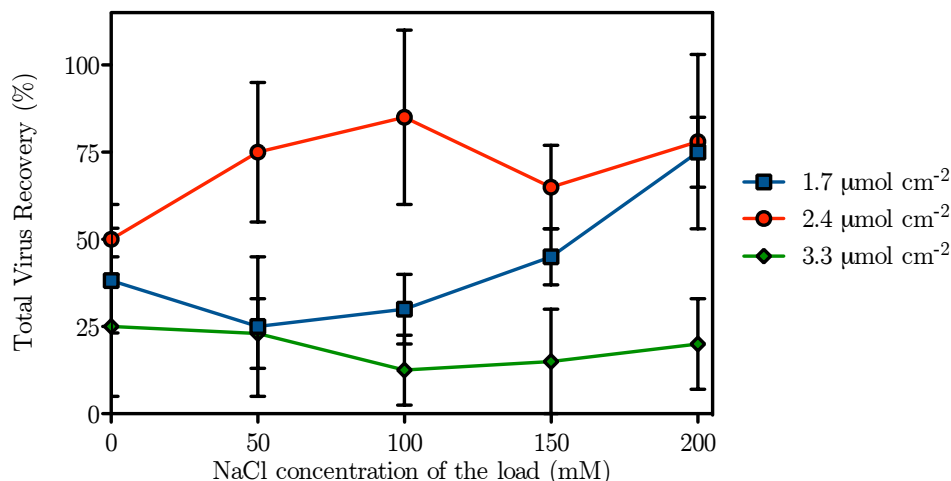


Figure 5.1: TP recovery after elution with 1 M NaCl for the hydrogel-grafted membrane with low, medium and high ligand density.

Ligand density has also been studied for mAb chromatography, where increased ligand density did not lead to improvements in binding capacity and recovery<sup>[138]</sup>. Therefore, it has been suggested that there is a threshold level above which ligand density does not improve matrix capacity<sup>[119,138]</sup>. However, the results herein presented show that increasing the ligand density above a certain threshold level not only did not increase virus recovery but also had a negative impact on virus recovery. This might be explained due to multi-point adsorption – leading to a stronger association between the virus and the membrane – or due to virus entrapment since, hydrogel layer thickness was increased in the highest ligand densities.

## 5.1.2 Impurity removal

### 5.1.2.1 Protein clearance

The total protein clearance obtained in the elution showed a slight increase with increased ionic strength. As expected, by increasing NaCl concentration of the load, it was possible to increase protein clearance for medium and high ligand densities (Figure 5.2). Also, the protein clearance increased concomitantly with increases in ligand density. The low protein clearance observed in the low ligand density ( $1.7 \mu\text{mol cm}^{-2}$ ) might be due to co-elution of proteins with the virus during the elution with 1 M NaCl. This problem can be addressed by the implementation of a gradient elution to improve resolution<sup>[119]</sup>.



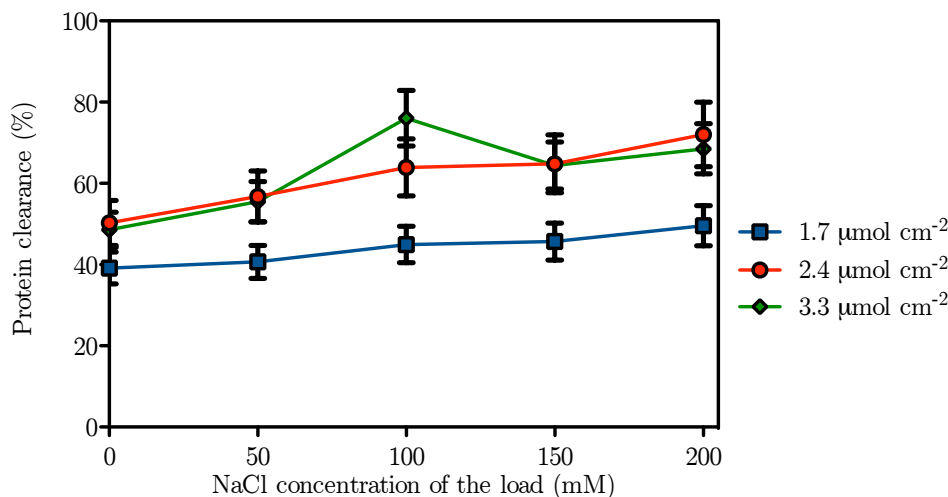


Figure 5.2: Protein clearance after elution with 1 M NaCl for the hydrogel-grafted membrane with low, medium and high ligand density.

#### 5.1.2.2 DNA clearance

DNA is an impurity whose removal poses some challenges because of its high affinity to the matrix; moreover, it can interact with the viruses. Considering the DNA clearance, no difference was observed between the different ligand densities assessed (Figure 5.3). Contrar-

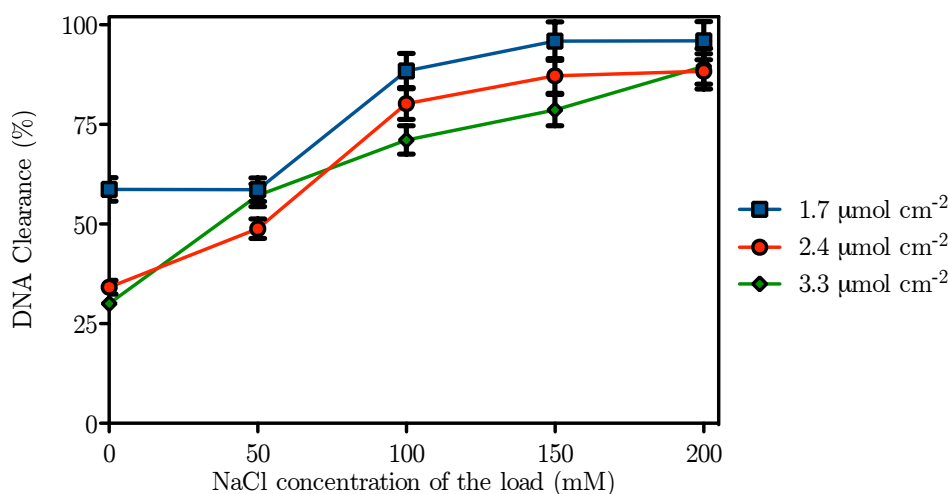


Figure 5.3: DNA clearance after elution with 1 M NaCl for the hydrogel-grafted membrane with low, medium and high ligand density.

ily, there was a notable increase in DNA clearance with increasing NaCl concentration in the 0–150 mM range. This suggests that increasing NaCl concentration in the load promotes DNA removal in the flow-through fraction. (The strongly associated DNA associated with the membrane was evaluated with 2 M NaCl elution and was found to be less than 7 %, data not shown.) This conductivity-dependent binding capacity is a well-know effect in AEX adsorption: at the solid-liquid interface the charged surface attracts counter-ions from the solution to form a "double layer" whose thickness is reduced with increasing ionic strength. A thin double layer reduces the biomolecule's contact area and thereby weakens and limits

the electrostatic interactions between the ion exchange group and the biomolecule resulting in reduced adsorption capacity<sup>[139,140]</sup>.

## 5.2 Directly grafted membranes

### 5.2.1 Virus recovery

With the directly grafted membrane virus binding was heavily reduced as can be observed by the high virus recovery in the flow-through and residual amounts eluted with 1 M NaCl (Figure 5.4). This is the opposite of what was observed in the hydrogel-grafted membranes,

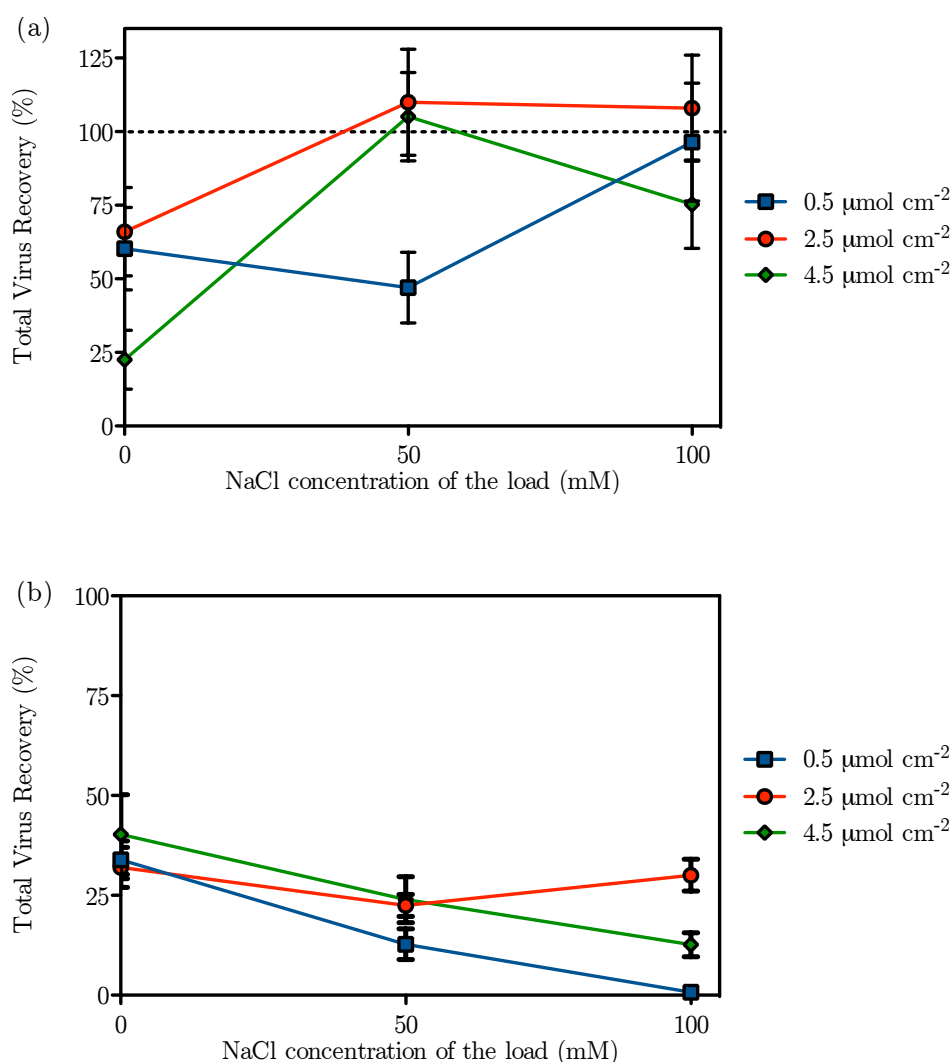


Figure 5.4: TP recovery (a) in the flow-through and (b) after elution with 1 M NaCl for the directly grafted membrane with low, medium and high ligand density.

despite the comparable ligand densities. As discussed previously, low conductivity promotes biomolecule binding leading to virus recovery in the flow-through between 23 and 66 % without NaCl. When the NaCl was increased to 50–100 mM the virus recovery was improved up to 100 % for the medium ligand density (2.5  $\mu\text{mol cm}^{-2}$ ).

Furthermore, in the experiments with the directly grafted membranes there was a good

agreement between the viruses in the flow-through and in the subsequent elution, corroborating the hypothesis that incomplete virus recovery in high ligand density is related with the hydrogel layer.

## 5.2.2 Impurity removal

### 5.2.2.1 Protein clearance

The analysis of total protein concentration in the flow-through did not show major differences between the 0.5 and 2.5  $\mu\text{mol cm}^{-2}$  ligand densities (Figure 5.5). The high ligand

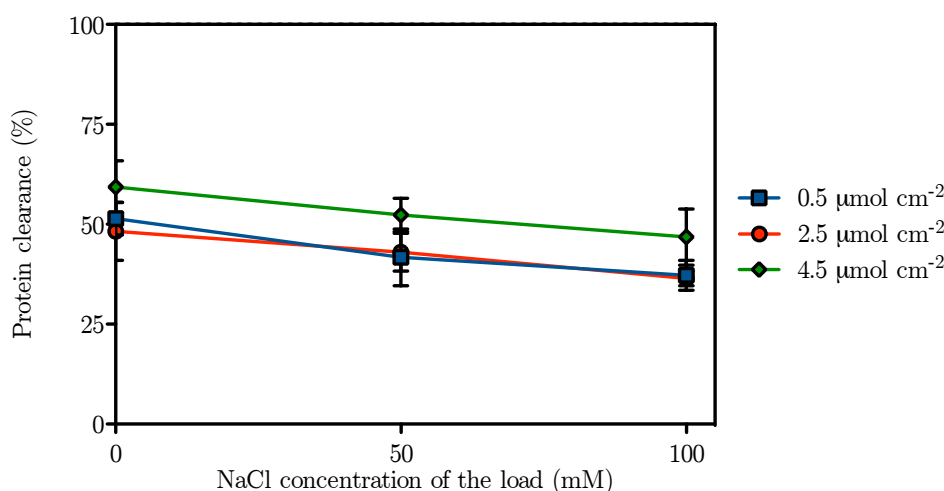


Figure 5.5: Protein clearance after elution with 1 M NaCl for the directly grafted membrane with low, medium and high ligand density.

density (4.5  $\mu\text{mol cm}^{-2}$ ) resulted in protein clearance slightly higher compared with the low and medium ligand densities assayed, suggesting an increase in protein binding capacity due to ligand density increase.

### 5.2.2.2 DNA clearance

In line with the results of HCP removal, loading with low conductivity resulted in higher DNA binding (and removal from flow-through) when compared with 50 and 100 mM of NaCl (Figure 5.6). The high and medium ligand density membranes seem to be more responsive to NaCl concentration. When using these membranes, conductivity increases led to lower DNA clearance in the flow-through fraction, meaning a decreased DNA binding (as observed previously, Figure 5.4). On the contrary, the low ligand density membrane shown a constant DNA clearance (56–58 %) within the NaCl concentration range tested.

Comparing the DNA clearance for both types of membrane structure, the results show that the hydrogel layer decrease accessibility of the DNA, resulting in high amounts of DNA in flow-through. Whereas the directly grafted membrane enabled DNA binding as proved by the 56–84 % DNA clearance in flow-through.

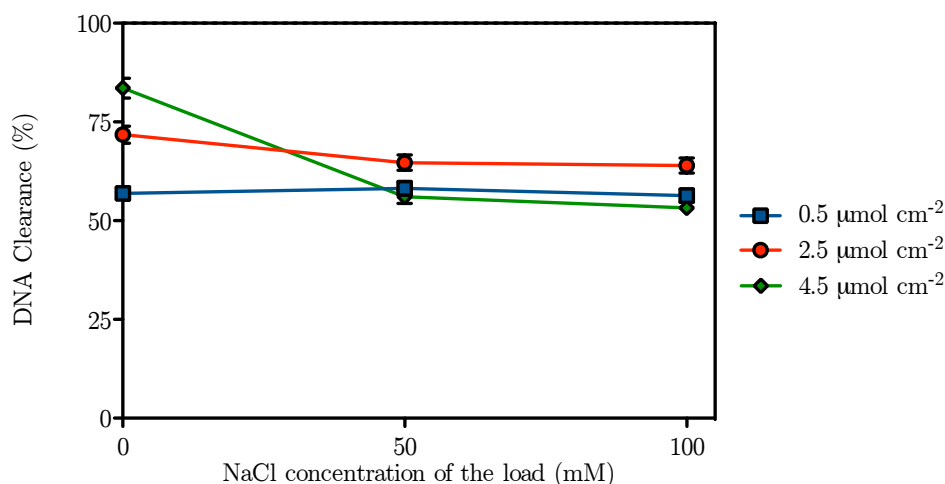


Figure 5.6: DNA clearance in the flow-through for the directly grafted membrane with low, medium and high ligand density.

### 5.3 Discussion

The membrane adsorbers were evaluated in bind/elute as well as flowthrough mode for purification of Ad5 from its process-derived impurities, such as DNA and total protein. A complex feed stock derived from bioreactor production was used in order to obtain a more realistic approach compared to other studies where model proteins or pure products are used<sup>[138,141]</sup>. In addition, the use of scale-down devices, such as the 96-well chromatographic system allows to screen several factors while characterizing the design space (Figure 5.7)

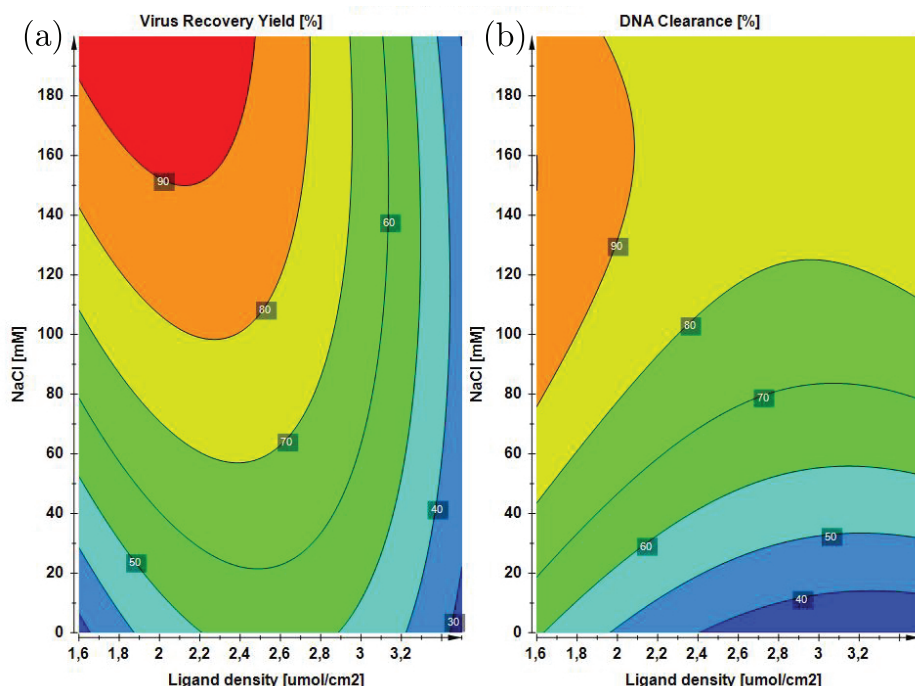


Figure 5.7: Experimental design space for the hydrogel-grafted membranes. The panel shows the (a) recovery yield and (b) DNA clearance of the 1 M NaCl elution for the hydrogel grafted membrane. A decreased ligand density and increased ionic strength to value of 150 mM NaCl are suitable conditions for hydrogel-grafted membranes.

The hydrogel-grafted membranes yield higher virus recoveries than the directly grafted membranes. Among the hydrogel-grafted membranes, lower and medium ligand densities improve the performance of the purification process. Particularly, the medium ligand density ( $2.4 \mu\text{mol cm}^{-2}$ ) appears to provide a good compromise between recovery yield (up to 85 %) and impurity removal (up to 96 % of DNA clearance).

The directly grafted membranes shown low virus binding leading to significant percentages of viruses in the flow-through, up to 100 %. Contrarily to the observed with the virus, the absence of hydrogel layer resulted in increased DNA binding and removal from the flow-through. Therefore, further improvements of these kind of membrane (for instance, by increasing ligand density) might lead to enhanced DNA removal and optimization of directly grafted membranes for polishing (flow-through) application.



## Part IV

# CONCLUSIONS





# General Discussion and Conclusion

Viruses and VLPs play an important role in the current medical therapies and have an enormous potential for the development of new applications in the fields of vaccination and gene therapy. However, the success of complex biopharmaceuticals deeply depends on the developers/manufacturers' capacity to deliver clinical-grade lots with a cost-effective manufacturing process. It must also guarantee a scalable and robust production delivering consistently the required product quality, safety and purity.

relies greatly on the manufacturing process. This process must guarantee a scalable and cost-effective production while achieving consistently the demanded product purity, safety and quality.

The upstream process has evolved substantially over the last few decades, on the opposite the downstream processing has been repeatedly identified as the bottleneck in the biopharmaceutical process<sup>[7,142]</sup>. Recent efforts have been made in order to improve the downstream processing, but its majority focused on the chromatographic separation with innovative supports<sup>[67,115]</sup>, column designs<sup>[120,121]</sup>, ligands<sup>[143]</sup> and operation modes<sup>[63,122]</sup>. This work illustrated how new and unexplored technologies can improve the productivity and efficiency of the entire DSP.

## 6.1 Debottlenecking the DSP right from the beginning

The upstream technology advances enabled high cell densities as part of process intensification efforts, however this and other improvements have created new challenges for bulk clarification<sup>[19,23]</sup>. In addition to the high biomass content, the large volumes must be processed quickly, especially when labile products are considered. The body feed filtration here evaluated is suggested as an alternative for bulk clarification (Chapter 3). The filter aid

trial enabled to select Divergan RS due to its superior Ad5 recovery. It is suggested that the non-charged nature of this synthetic polymer combined with its high specific area are responsible for the superior performance compared with the remaining DE assessed. Further developments and integration into a scalable filtration set-up will render body feed filtration as an alternative to depth filter clarification<sup>[77,82]</sup>.

Ultrafiltration is a unit operation widely used in pilot- and industrial-scale purification schemes<sup>[19,22,106]</sup>. Ultrafiltration can be applied to concentrate a bulk and/or to exchange buffer in a scalable manner. The majority of the literature reports the use of HF modules which are associated with lower shear rates but longer processing times when compared with the flat-sheet cassette modules. In this work several cassette and HF modules were compared for Ad5 and RV concentration and buffer exchange (Chapter 4). Our results indicate that large cut-off cassette modules are suitable to Ad5 concentration with complete IP recoveries in shorter processing times compared with currently available hollow fibers.

Chromatography, especially IEX chromatography, is a well-established operation for virus purification due to its separation power and versatility<sup>[7,68]</sup>. Traditionally chromatography has been performed with packed-bed columns, however new stationary phases, such as membrane adsorbers, have several advantages capable of improving chromatography productivity by decreasing processing times and buffer usage. Furthermore, the low production cost enables the use of membrane adsorbers as single-use devices, avoiding regeneration, CIP and validation procedures. The work developed in this thesis demonstrates how specific membrane features (*i. e.* ligand density and membrane structure) together with load conductivity impact binding and purification of an Adenovirus model (Chapter 5). Our results demonstrate that a grafted membrane with a ligand density of  $2.4 \mu\text{mol cm}^{-2}$  provided the best trade-off between high virus recovery and high DNA removal, when operated in bind/elute mode. In addition, the use of a 96-well system enabled a high-throughput screening in a Design of Experiments (DoE) approach.

## 6.2 Future work and outlook

This thesis' work led to the identification of innovative technologies capable of improving the current viruses DSP, however further optimizations are required. The body feed filtration should be implemented in a scalable set-up in order to confirm this novel technology as an alternative for clarification. Further developments should target the characterization of the intrinsic filter aid material permeability (with pure water), conductivity adjustments and addition of flocculants (domiphen bromide) or precipitants (*e. g.*  $(\text{NH}_4)_3\text{SO}_4$ ) to increase filtration performance. Additionally, the determination of particle size, size distribution and  $\zeta$ -potential of the filter aid material (and virus bulk) would provide valuable information to understand the interaction mechanism. Ultrafiltration using large MWCO cassette modules was successfully employed to concentrate Ad5, but the low recoveries observed for RV indicate that further optimizations are needed specially for low-titer and shear-sensitive viruses. The following work should target the optimization of MWCO, shear rate and membrane load. Also, it should be determined if increasing diafiltration buffer enables to increase the recovery yield of this step. Considering the membrane adsorbers used for IEX chromatography, the

determination of the dynamic binding capacity for viruses as well as for the main impurities would be a valuable information towards a rational process development of the chromatographic step. Such information could be later incorporated in the design of continuous or semi-continuous chromatography operation.

The ultimate goal for DSP is to have a robust purification platform running continuously delivering the required purity. Considering this goal, disposable devices (depth filters or ultrafiltration devices) will be helpful in early steps of the DSP<sup>[60,62]</sup>, however chromatographic separation still needs further development. In this context, continuous or semi-continuous chromatography routines that have been suggested for mAbs might be applied also for virus purification<sup>[63,144,145]</sup>. Besides continuous operation, convective mass transport chromatographic supports like membrane adsorbers and monoliths can further enhance the productivity of chromatography<sup>[114,115]</sup>. Combination of these established technologies with old separation technologies, such as precipitation and aqueous two-phase systems, could render new and improved DSP schemes; however the feasibility of such revisited technologies must be confirmed specifically for virus purification<sup>[100,103,116,146]</sup>.

Following the Quality by Design (QbD) initiative launched by the FDA and International Conference on Harmonization (ICH)<sup>[147]</sup>, scale-down tools that enable knowledge-based process development<sup>[148,149]</sup> and improved analytical assays will be increasingly important<sup>[150–153]</sup>.



# Bibliography

1. Josefsberg, J.O., Buckland, B.. Vaccine process technology. *Biotechnol Bioeng* 2012; **109**(6):1443–1460.
2. Walsh, G.. Biopharmaceutical benchmarks 2010. *Nat Biotechnol* 2010; **28**(9):917–924.
3. Declerck, P.. Biologicals and biosimilars: a review of the science and its implications. *GaBI J* 2012; **1**(1):13–16.
4. Burnett, J.R., Hooper, A.J.. Alipogene tiparvovec, an adeno-associated virus encoding the Ser(447)X variant of the human lipoprotein lipase gene for the treatment of patients with lipoprotein lipase deficiency. *Curr Opin Mol Ther* 2009; **11**(6):681–691.
5. Roldão, A., Mellado, M.C.M., Castilho, L.R., Carrondo, M.J., Alves, P.M.. Virus-like particles in vaccine development. *Expert Rev Vaccines* 2010; **9**(10):1149–1176.
6. El-Aneed, A.. An overview of current delivery systems in cancer gene therapy. *J Control Release* 2004; **94**(1):1–14.
7. Wolff, M.W., Reichl, U.. Downstream processing of cellculture-derived virus particles. *Expert Rev Vaccines* 2011; **10**(10):1451–1475.
8. Noad, R., Roy, P.. Virus-like particles as immunogens. *Trends Microbiol* 2003; **11**(9):438–444.
9. Abdel-Motal, U.M., Guay, H.M., Wigglesworth, K., Welsh, R.M., Galili, U.. Immunogenicity of influenza virus vaccine is increased by anti-gal-mediated targeting to antigen-presenting cells. *J Virol* 2007; **81**(17):9131–9141.
10. Wang, W., Lu, B., Zhou, H., Suguitan, A.L., Cheng, X., Subbarao, K., et al. Glycosylation at 158N of the Hemagglutinin Protein and Receptor Binding Specificity Synergistically Affect the Antigenicity and Immunogenicity of a Live Attenuated H5N1 A/Vietnam/1203/2004 Vaccine Virus in Ferrets. *J Virol* 2010; **84**(13):6570–6577.

11. Heilbronn, R., Weger, S.. Viral Vectors for Gene Transfer: Current Status of Gene Therapeutics. In: Schäfer-Korting, M., editor. *Handbook of Experimental Pharmacology*. Berlin: Springer Verlag Berlin Heidelberg; 2009, p. 143–170.
12. Bae, K., Choi, J., Jang, Y., Ahn, S., Hur, B.. Innovative vaccine production technologies: the evolution and value of vaccine production technologies. *Arch Pharm Res* 2009; **32**(4):465–480.
13. Fahim, R.E.F., Tan, L.U.L., Barreto, L., Thipphawong, J., Jackson, G.E.D.. Multivalent DTP-Polio vaccines. *European Patent 1762246 A1* 2007;.
14. Klade, C., Scharnagl, N.. Japanese encephalitis virus (JEV) and tick-borne encephalitis virus (TBEV) peptides stimulating human T-cell responses. *World Patent 024534 A2* 2009;.
15. Friedman, P.A., Krah, D.A., Provost, P.J.. Process for attenuated varicella zoster virus vaccine production. *European Patent 0573107 B1* 1993;.
16. Liu, J., Schwartz, R., Thompson, M., Maranga, L.J.C., HSU, S.S.T., Ghosh, M., et al. MDCK cell lines supporting viral growth to high titers and bioreactor process using the same. *US Patent 0052717 A1* 2013;.
17. de Vocht, M.L., Veenstra, M.. Process for adenovirus purification from high cell density cultures. *US Patent 0202268 A1* 2012;.
18. Luitjens, A., van Herk, H.. Method for the production of Ad26 adenoviral vectors. *US Patent 0315696 A1* 2012;.
19. Altaras, N.E., Aunins, J.G., Evans, R.K., Kamen, A., Konz, J.O., Wolf, J.J.. Production and formulation of adenovirus vectors. *Adv Biochem Eng Biotechnol* 2005; **99**:193–260.
20. Le Ru, A., Jacob, D., Transfiguracion, J., Ansorge, S., Henry, O., Kamen, A.A.. Scalable production of influenza virus in HEK-293 cells for efficient vaccine manufacturing. *Vaccine* 2010; **28**(21):3661–3671.
21. Cook, J.C.. Process for purifying human papillomavirus virus-like particles. *World Patent 2000009671 A1* 2000;.
22. Descamps, D., Giannini, S., Lecrenier, N., Stephenne, J., Wettendorff, M.A.C.. Vaccine against HPV. *US Patent 0189229 A1* 2011;.
23. Silva, A.C., Peixoto, C., Lucas, T., Küppers, C., Cruz, P.E., Alves, P.M., et al. Adenovirus vector production and purification. *Curr Gene Ther* 2010; **10**(6):437–455.
24. Kotin, R.M.. Large-scale recombinant adeno-associated virus production. *Hum Mol Genet* 2011; **20**(R1):R2–R6.
25. Urabe, M., Ozawa, K., Haast, S.J.P., Hermens, W.T.J.M.C.. Adv vectors produced in insect cells. *US Patent 8163543 B2* 2013;.

26. Coroadinha, A.S., Gama-Norton, L., Amaral, A.I., Hauser, H., Alves, P.M., Cruz, P.E.. Production of retroviral vectors: review. *Curr Gene Ther* 2010; **10**(6):456–473.
27. Rodrigues, A.F., Alves, P.M., Coroadinha, A.S.. Production of Retroviral and Lentiviral Gene Therapy Vectors: Challenges in the Manufacturing of Lipid Enveloped Virus. In: Xu, K., editor. *Viral Gene Therapy*. INTECH; 2011, p. 15–40.
28. Specifications: test procedures and acceptance criteria for biotechnological/biological products. *ICH Q6B* 1999;.
29. Viral safety evaluation of biotechnology products derived from cell lines of human or animal origin. *ICH Q5A(R1)* 1999;.
30. Evaluation and recommendation of pharmacopoeial texts for use in the ICH regions. *ICH Q4B* 2007;.
31. Dolgin, E.. Gene therapies advance, but some see manufacturing challenges. *Nat Med* 2012; **18**(12):1718–1719.
32. Stewart, P.L.. Adenovirus structure. In: Curiel, D.T., Douglas, J.T., editors. *Adenoviral Vectors for Gene Therapy*. San Diego: Academic Press; 2002, p. 1–18.
33. Horne, R.W., Brenner, S., Waterson, A.P., Wildy, P.. The icosahedral form of an adenovirus. *J Mol Biol* 1959; **1**(1):84–86.
34. Ruigrok, R.W., Nermut, M.V., Andree, P.J.. The molecular mass of adenovirus type 5 as determined by means of scanning transmission electron microscopy (STEM). *J Virol Methods* 1984; **9**(1):69–78.
35. Russell, W.C.. Adenoviruses: update on structure and function. *Journal of General Virology* 2009; **90**(1):1–20.
36. Trilisky, E.I., Lenhoff, A.M.. Sorption processes in ion-exchange chromatography of viruses. *J Chromatogr A* 2007; **1142**(1):2–12.
37. Roitsch, C., Achstetter, T., Bendaib, M., Bonfils, E., Cauet, G., Gloeckler, R., et al. Characterization and quality control of recombinant adenovirus vectors for gene therapy. *J Chromatogr B Biomed Sci Appl* 2001; **752**(2):263–280.
38. Blanche, F., Monegier, B., Faucher, D., Duchesne, M., Audhuy, F., Barbot, A., et al. Polypeptide composition of an adenovirus type 5 used in cancer gene therapy. *J Chromatogr A* 2001; **921**(1):39–48.
39. Rux, J.J., Burnett, R.M.. Adenovirus structure. *Hum Gene Ther* 2004; **15**(12):1167–1176.
40. de Vrij, J., Willemsen, R.A., Lindholm, L., Hoeben, R.C., GIANT Consortium, Bangma, C.H., et al. Adenovirus-derived vectors for prostate cancer gene therapy. *Hum Gene Ther* 2010; **21**(7):795–805.

41. Zhang, Y., Fang, L., Zhang, Q., Zheng, Q., Tong, J., Fu, X., et al. An oncolytic adenovirus regulated by a radiation-inducible promoter selectively mediates hSulf-1 gene expression and mutually reinforces antitumor activity of I(131)-metuximab in hepatocellular carcinoma. *Mol Oncol* 2013; **7**(3):346–358.
42. Barouch, D.H.. Novel adenovirus vector-based vaccines for HIV-1. *Curr Opin HIV AIDS* 2010; **5**(5):386–390.
43. Schuldt, N.J., Amalfitano, A.. Malaria vaccines: Focus on adenovirus based vectors. *Vaccine* 2012; **30**(35):5191–5198.
44. Ma, G., Shimada, H., Hiroshima, K., Tada, Y., Suzuki, N., Tagawa, M.. Gene medicine for cancer treatment: Commercially available medicine and accumulated clinical data in China. *Drug Des Devel Ther* 2008; **2**:115.
45. Rätty, J.K., Pikkarainen, J.T., Wirth, T., Ylä-Herttua, S.. Gene therapy: the first approved gene-based medicines, molecular mechanisms and clinical indications. *Curr Mol Pharmacol* 2008; **1**(1):13–23.
46. Barouch, D.H., Nabel, G.J.. Adenovirus vector-based vaccines for human immunodeficiency virus type 1. *Hum Gene Ther* 2005; **16**(2):149–156.
47. Esparza, J.. Progress in the development of an adenovirus 26 vector platform for HIV vaccines. *Expert Rev Vaccines* 2013; **12**(5):477–480.
48. Giacca, M., Zacchigna, S.. Virus-mediated gene delivery for human gene therapy. *J Control Release* 2012; **161**(2):377–388.
49. Tatsis, N., Ertl, H.C.J.. Adenoviruses as vaccine vectors. *Mol Ther* 2004; **10**(4):616–629.
50. Coffin, J.M.. Structure and classification of Retrovirus. In: Levy, J.a., editor. *The retroviridae*. New York: Academic Press; 1992, p. 19–49.
51. Andreadis, S.T., Roth, C.M., Le Doux, J.M., Morgan, J.R., Yarmush, M.L.. Large-Scale Processing of Recombinant Retroviruses for Gene Therapy. *Biotechnol Prog* 1999; **15**(1):1–11.
52. Rein, A.. Murine Leukemia Viruses: Objects and Organisms. *Adv Virol* 2011; **2011**(1):1–14.
53. Ginn, S.L., Alexander, I.E., Edelstein, M.L., Abedi, M.R., Wixon, J.. Gene therapy clinical trials worldwide to 2012 - an update. *J Gene Med* 2013; **15**(2):65–77.
54. Carrondo, M., Panet, A., Wirth, D., Coroadinha, A.S., Cruz, P., Falk, H., et al. Integrated Strategy for the Production of Therapeutic Retroviral Vectors. *Hum Gene Ther* 2011; **22**(3):370–379.



55. Eckert, H.G., Kühlcke, K., Schilz, A.J., Lindemann, C., Basara, N., Fauser, A.A., et al. Clinical scale production of an improved retroviral vector expressing the human multidrug resistance 1 gene (MDR1). *Bone Marrow Transplant* 2000; **25**(S2):S114–S117.
56. Przybylowski, M., Hakakha, A., Stefanski, J., Hodges, J., Sadelain, M., Rivière, I.. Production scale-up and validation of packaging cell clearance of clinical-grade retroviral vector stocks produced in Cell Factories. *Gene Ther* 2006; **13**(1):95–100.
57. Wikström, K., Blomberg, P., Islam, K.B.. Clinical grade vector production: analysis of yield, stability, and storage of gmp-produced retroviral vectors for gene therapy. *Biotechnol Prog* 2004; **20**(4):1198–1203.
58. Shukla, A.A., Hubbard, B., Tressel, T., Guhan, S., Low, D.. Downstream processing of monoclonal antibodies—Application of platform approaches. *J Chromatogr B* 2007; **848**(1):28–39.
59. Roque, A.C.A., Lowe, C.R., Taipa, M.A.. Antibodies and Genetically Engineered Related Molecules: Production and Purification. *Biotechnol Prog* 2004; **20**(3):639–654.
60. Gottschalk, U.. Disposables in downstream processing. *Adv Biochem Eng Biotechnol* 2010; **115**:171–183.
61. Kuczewski, M., Schirmer, E., Lain, B., Zarbis-Papastoitsis, G.. A single-use purification process for the production of a monoclonal antibody produced in a PER.C6 human cell line. *Biotechnol J* 2010; **6**(1):56–65.
62. Shukla, A.A., Gottschalk, U.. Single-use disposable technologies for biopharmaceutical manufacturing. *Trends Biotechnol* 2013; **31**(3):149–156.
63. Godawat, R., Brower, K., Jain, S., Konstantinov, K., Riske, F., Warikoo, V.. Periodic counter-current chromatography - design and operational considerations for integrated and continuous purification of proteins. *Biotechnol J* 2012; **7**(12):1496–1508.
64. Warikoo, V., Godawat, R., Brower, K., Jain, S., Cummings, D., Simons, E., et al. Integrated continuous production of recombinant therapeutic proteins. *Biotechnol Bioeng* 2012; **109**(12):3018–3029.
65. Zhang, S., Thwin, C., Wu, Z., Cho, T., Wilson, D., Caston, L.. Methods for producing purified adenoviral vectors. *US Patent 7510875 B2* 2009;.
66. Peixoto, C., Ferreira, T.B., Sousa, M.F.Q., Carrondo, M.J.T., Alves, P.M.. Towards purification of adenoviral vectors based on membrane technology. *Biotechnol Prog* 2008; **24**(6):1290–1296.
67. Fernandes, P., Peixoto, C., Santiago, V.M., Kremer, E.J., Coroadinha, A.S., Alves, P.M.. Bioprocess development for canine adenovirus type 2 vectors. *Gene Ther* 2012; **20**(4):353–360.

68. Segura, M.M., Kamen, A.A., Garnier, A.. Overview of Current Scalable Methods for Purification of Viral Vectors. In: Merten, O.W., Al-Rubeai, M., editors. *Viral Vectors for Gene Therapy: Methods and Protocols*. Totowa, NJ: Humana Press; 2011, p. 89–116.
69. Vicente, T., Peixoto, C., Carrondo, M.J.T., Alves, P.M.. Purification of recombinant baculoviruses for gene therapy using membrane processes. *Gene Ther* 2009; **16**(6):766–775.
70. Goerke, A.R., To, B.C.S., Lee, A.L., Sagar, S.L., Konz, J.O.. Development of a novel adenovirus purification process utilizing selective precipitation of cellular DNA. *Biotechnol Bioeng* 2005; **91**(1):12–21.
71. Konz, J.O., Lee, A.L., To, B.C.S., Goerke, A.R.. Methods of adenovirus purification. *US Patent 0118970 A1* 2008;.
72. Konz, J.O., Lee, A.L., Lewis, J.A., Sagar, S.L.. Development of a purification process for adenovirus: controlling virus aggregation to improve the clearance of host cell DNA. *Biotechnol Prog* 2005; **21**(2):466–472.
73. Russell, E., Wang, A., Rathore, A.S.. Harvest of a Therapeutic Protein Product from High Cell Density Fermentation Broths: Principles and Case Study. In: Shukla, A.A., Etzel, M.R., Gadam, S., editors. *Process Scale Bioseparations for the Biopharmaceutical Industry*. Boca Raton: CRC Press; 2007, p. 1–58.
74. Liu, H.F., Ma, J., Winter, C., Bayer, R.. Recovery and purification process development for monoclonal antibody production. *MAbs* 2010; **2**(5):480–499.
75. Kelley, B.. Very Large Scale Monoclonal Antibody Purification: The Case for Conventional Unit Operations. *Biotechnol Prog* 2007; **23**:995–1008.
76. Chon, J.H., Zarbis-Papastoitsis, G.. Advances in the production and downstream processing of antibodies. *N Biotechnol* 2011; **28**(5):458–463.
77. Roush, D.J., Lu, Y.. Advances in Primary Recovery: Centrifugation and Membrane Technology. *Biotechnol Prog* 2008; **24**(3):488–495.
78. Ostreicher, E.A., Arnold, T.E., Conway, R.S.. Charge Modified Filter Media. In: Jornitz, M.W., Meltzer, T.H., editors. *Filtration and Purification in the Biopharmaceutical Industry*. Informa Healthcare; 2008, p. 23–46.
79. Kalbfuss, B., Genzel, Y., Wolff, M., Zimmermann, A., Morenweiser, R., Reichl, U.. Harvesting and concentration of human influenza A virus produced in serum-free mammalian cell culture for the production of vaccines. *Biotechnol Bioeng* 2007; **97**(1):73–85.
80. Peixoto, C., Sousa, M.F.Q., Silva, A.C., Carrondo, M.J.T., Alves, P.M.. Downstream processing of triple layered rotavirus like particles. *J Biotechnol* 2007; **127**(3):452–461.

81. Yigzaw, Y., Piper, R., Tran, M., Shukla, A.A.. Exploitation of the adsorptive properties of depth filters for host cell protein removal during monoclonal antibody purification. *Biotechnol Prog* 2006; **22**(1):288–296.
82. Singh, N., Pizzelli, K., Romero, J.K., Chrostowski, J., Evangelist, G., Hamzik, J., et al. Clarification of recombinant proteins from high cell density mammalian cell culture systems using new improved depth filters. *Biotechnol Bioeng* 2013; **110**(7):1964–1972.
83. Rodrigues, T., Carvalho, A., Carmo, M., Carrondo, M.J.T., Alves, P.M., Cruz, P.E.. Scaleable purification process for gene therapy retroviral vectors. *J Gene Med* 2007; **9**(4):233–243.
84. van Reis, R., Zydney, A.. Bioprocess membrane technology. *J Memb Sci* 2007; **297**(1-2):16–50.
85. Jonas, F., Diel, B.. Device and method for filtering a liquid sample. *World Patent 2013034242 A1* 2013;.
86. Koehler, K., Tarrach, K., Thiefes, A.. Depth filter layer with inorganic layer double hydroxide. *US Patent 0207196 A1* 2011;.
87. Freeman, G.J., McKechnie, M.T.. Filtration and Stabilization of Beers. In: Lea, A.G.H., Piggott, J.R., editors. *Fermented Beverage Production*. Springer; 2003, p. 365–392.
88. Thomassen, Y.E., van 't Oever, A.G., Vinke, M., Spiekstra, A., Wijffels, R.H., van der Pol, L.A., et al. Scale-down of the inactivated polio vaccine production process. *Biotechnol Bioeng* 2013; **110**(5):1354–1365.
89. Farid, S.S.. Process economics of industrial monoclonal antibody manufacture. *J Chromatogr B Analyt Technol Biomed Life Sci* 2007; **848**(1):8–18.
90. Zydney, A.L.. Membrane technology for purification of therapeutic proteins. *Biotechnol Bioeng* 2009; **103**(2):227–230.
91. van Reis, R., Zydney, A.. Membrane processes in biotechnology: An overview. *Biotechnol Adv* 2006; **24**(5):482–492.
92. Segura, M.M., Mangion, M., Gaillet, B., Garnier, A.. New developments in lentiviral vector design, production and purification. *Expert Opin Biol Ther* 2013; **13**(7):987–1011.
93. Bandeira, V.S., Peixoto, C., Rodrigues, A.F., Cruz, P., Alves, P., Coroadinha, A.S., et al. Downstream Processing of Lentiviral Vectors: releasing bottlenecks. *Hum Gene Ther Methods* 2012; **23**(4):255–263.
94. Kamen, A., Henry, O.. Development and optimization of an adenovirus production process. *J Gene Med* 2004; **6**(S1):S184–S192.

95. Segura, M.M., Puig, M., Monfar, M., Chillón, M.. Chromatography Purification of Canine Adenoviral Vectors. *Hum Gene Ther Methods* 2012; **23**(3):182–197.
96. Wickramasinghe, S.R., Kalbfuß, B., Zimmermann, A., Thom, V., Reichl, U.. Tangential flow microfiltration and ultrafiltration for human influenza A virus concentration and purification. *Biotechnol Bioeng* 2005; **92**(2):199–208.
97. Subramanian, S., Altaras, G.M., Chen, J., Hughes, B.S., Zhou, W., Altaras, N.E.. Pilot-Scale Adenovirus Seed Production through Concurrent Virus Release and Concentration by Hollow Fiber Filtration. *Biotechnol Prog* 2008; **21**(3):851–859.
98. Weggeman, M., van Corven, E.J.J.M.. Virus purification methods. *European Patent 1780269 B1* 2005;.
99. Rodrigues, T., Carrondo, M.J.T., Alves, P.M., Cruz, P.E.. Purification of retroviral vectors for clinical application: Biological implications and technological challenges. *J Biotechnol* 2007; **127**(3):520–541.
100. Oelmeier, S.A., Dismar, F., Hubbuch, J.. Application of an aqueous two-phase systems high-throughput screening method to evaluate mAb HCP separation. *Biotechnol Bioeng* 2010; **108**(1):69–81.
101. Azevedo, A.M., Rosa, P.A.J., Ferreira, I.F., Aires-Barros, M.R.. Optimisation of aqueous two-phase extraction of human antibodies. *J Biotechnol* 2007; **132**(2):209–217.
102. Gervais, D.P., Pfeiffer, K.A.. Antibody purification process by precipitation. *US Patent 0204455 A1* 2010;.
103. Knevelman, C., Davies, J., Allen, L., Titchener-Hooker, N.J.. High-throughput screening techniques for rapid PEG-based precipitation of IgG4 mAb from clarified cell culture supernatant. *Biotechnol Prog* 2009; **26**(3):697–705.
104. McDonald, P., Victa, C., Carter-Franklin, J.N., Fahrner, R.. Selective antibody precipitation using polyelectrolytes: A novel approach to the purification of monoclonal antibodies. *Biotechnol Bioeng* 2009; **102**(4):1141–1151.
105. Benavides, J., Mena, J.A., Cisneros-Ruiz, M., Ramírez, O.T., Palomares, L.A., Rito-Palomares, M.. Rotavirus-like particles primary recovery from insect cells in aqueous two-phase systems. *J Chromatogr B Analyt Technol Biomed Life Sci* 2006; **842**(1):48–57.
106. Vicente, T., Roldão, A., Peixoto, C., Carrondo, M.J.T., Alves, P.M.. Large-scale production and purification of VLP-based vaccines. *J Invertebr Pathol* 2011; **107**(S):S42–S48.
107. Wolff, M.W., Siewert, C., Hansen, S.P., Faber, R., Reichl, U.. Purification of cell culture-derived modified vaccinia ankara virus by pseudo-affinity membrane adsorbers and hydrophobic interaction chromatography. *Biotechnol Bioeng* 2010; **107**(2):312–320.

108. Riske, F., Berard, N., Albee, K., Pan, P., Henderson, M., Adams, K., et al. Development of a platform process for adenovirus purification that removes human SET and nucleolin and provides high purity vector for gene delivery. *Biotechnol Bioeng* 2013; **110**(3):848–856.
109. Shabram, P.W., Giroux, D.D., Goudreau, A.M., Gregory, R.J., Horn, M.T., Huyghe, B.G., et al. Analytical anion-exchange HPLC of recombinant type-5 adenoviral particles. *Hum Gene Ther* 1997; **8**(4):453–465.
110. Konz, J.O., Livingood, R.C., Bett, A.J., Goerke, A.R., Laska, M.E., Sagar, S.L.. Serotype specificity of adenovirus purification using anion-exchange chromatography. *Hum Gene Ther* 2005; **16**(11):1346–1353.
111. Kuhn, I., Larsen, B., Gross, C., Hermiston, T.. High-performance liquid chromatography method for rapid assessment of viral particle number in crude adenoviral lysates of mixed serotype. *Gene Ther* 2007; **14**(2):180–184.
112. Ghosh, R.. Protein separation using membrane chromatography: opportunities and challenges. *J Chromatogr A* 2002; **952**(1-2):13–27.
113. Rathore, A.S., Shirke, A.. Recent developments in membrane-based separations in biotechnology processes: review. *Prep Biochem Biotechnol* 2011; **41**(4):398–421.
114. Orr, V., Zhong, L., Moo-Young, M., Chou, C.P.. Recent advances in bioprocessing application of membrane chromatography. *Biotechnol Adv* 2013; **31**(4):450–465.
115. Jungbauer, A., Hahn, R.. Polymethacrylate monoliths for preparative and industrial separation of biomolecular assemblies. *J Chromatogr A* 2008; **1184**(1-2):62–79.
116. Gottschalk, U., Brorson, K., Shukla, A.A.. Innovation in biomanufacturing: the only way forward. *Pharm Bioprocess* 2013; **1**(2):141–157.
117. Eglon, M.N., Duffy, A.M., O'Brien, T., Strappe, P.M.. Purification of adenoviral vectors by combined anion exchange and gel filtration chromatography. *J Gene Med* 2009; **11**(11):978–989.
118. Weaver, J., Husson, S.M., Murphy, L., Wickramasinghe, S.R.. Anion exchange membrane adsorbers for flow-through polishing steps: Part II. Virus, host cell protein, DNA clearance, and antibody recovery. *Biotechnol Bioeng* 2013; **110**(2):500–510.
119. Vicente, T., Faber, R., Alves, P.M., Carrondo, M.J.T., Mota, J.P.B.. Impact of ligand density on the optimization of ion-exchange membrane chromatography for viral vector purification. *Biotechnol Bioeng* 2011; **108**(6):1347–1359.
120. Cabanne, C., Raedts, M., Zavadzky, E., Santarelli, X.. Evaluation of radial chromatography versus axial chromatography, practical approach. *J Chromatogr B* 2007; **845**(2):191–199.

121. Besselink, T., van der Padt, A., Janssen, A.E.M., Boom, R.M.. Are axial and radial flow chromatography different? *J Chromatogr A* 2013; **1271**(1):105–114.
122. Mahajan, E., George, A., Wolk, B.. Improving affinity chromatography resin efficiency using semi-continuous chromatography. *J Chromatogr A* 2012; **1227**:154–162.
123. Guiochon, G., Beaver, L.A.. Separation science is the key to successful biopharmaceuticals. *J Chromatogr A* 2011; **1218**(49):8836–8858.
124. Evans, R.K., Nawrocki, D.K., Isopi, L.A., Williams, D.M., Casimiro, D.R., Chin, S., et al. Development of stable liquid formulations for adenovirus-based vaccines. *J Pharm Sci* 2004; **93**(10):2458–2475.
125. Cruz, P.E., Silva, A.C., Roldao, A., Carmo, M., Carrondo, M.J.T., Alves, P.M.. Screening of Novel Excipients for Improving the Stability of Retroviral and Adenoviral Vectors. *Biotechnol Prog* 2006; **22**(2):568–576.
126. Burden, C.S., Jin, J., Podgornik, A., Bracewell, D.G.. A monolith purification process for virus-like particles from yeast homogenate. *J Chromatogr B* 2012; **880**:82–89.
127. Coroadinha, A.S., Schucht, R., Gama-Norton, L., Wirth, D., Hauser, H., Carrondo, M.J.T.. The use of recombinase mediated cassette exchange in retroviral vector producer cell lines: Predictability and efficiency by transgene exchange. *J Biotechnol* 2006; **124**(2):457–468.
128. Kestin, J., Sokolov, M., Wakeham, W.A.. Viscosity of Liquid Water in the Range -8°C to 150°C. *J Phys Chem Ref Data* 1978; **7**(3):941–948.
129. Cheryan, M.. Performance and engineering models. In: Cheryan, M., editor. *Ultrafiltration and Microfiltration Handbook*. Lancaster: Taylor & Francis; 1998, p. 113–170.
130. Kennedy, M.A., Parks, R.J.. Adenovirus Virion Stability and the Viral Genome: Size Matters. *Mol Ther* 2009; **17**(10):1664–1666.
131. Rexroad, J., Evans, R.K., Middaugh, C.R.. Effect of pH and ionic strength on the physical stability of adenovirus type 5. *Biotechnol Bioeng* 2005; **95**(2):237–247.
132. Comparing Conventional Diatomite and Celpure® Filter Aids, [http://www.advancedminerals.com/pdf/AMC02\\_Compare\\_Conv.\\_F.\\_Aid\\_Celpure.pdf](http://www.advancedminerals.com/pdf/AMC02_Compare_Conv._F._Aid_Celpure.pdf). accessed 20th August 2013;.
133. Liu, H.F., McCooey, B., Duarte, T., Myers, D.E., Hudson, T., Amanullah, A., et al. Exploration of overloaded cation exchange chromatography for monoclonal antibody purification. *J Chromatogr A* 2011; **1218**(39):6943–6952.
134. About Divergan, [http://www.crosspure.basf.com/web/global/crosspure/en\\_GB/about\\_divergan/index](http://www.crosspure.basf.com/web/global/crosspure/en_GB/about_divergan/index). accessed 20th August 2013;.

135. Kuiper, M., Sanches, R.M., Walford, J.A., Slater, N.K.H.. Purification of a functional gene therapy vector derived from Moloney murine leukaemia virus using membrane filtration and ceramic hydroxyapatite chromatography. *Biotechnol Bioeng* 2002; **80**(4):445–453.
136. Silva, A.C., Simão, D., Sousa, M.F.Q., Peixoto, C., Cruz, P., Carrondo, M.J.T., et al. Production and purification of Ad vectors: current status and future needs for Adenovirus vector production. In: Cohen-Haguenauer, O., editor. *The CliniBook: Clinical gene transfer state of the art*. Paris: EDK; 2012, p. 245–250.
137. Cruz, P.E., Goncalves, D., Almeida, J., Moreira, J.L., Carrondo, M.J.T.. Modeling Retrovirus Production for Gene Therapy. 2. Integrated Optimization of Bioreaction and Downstream Processing. *Biotechnol Prog* 2000; **16**(3):350–357.
138. Hardin, A.M., Harinarayan, C., Malmquist, G., Axén, A., van Reis, R.. Ion exchange chromatography of monoclonal antibodies: effect of resin ligand density on dynamic binding capacity. *J Chromatogr A* 2009; **1216**(20):4366–4371.
139. Okada, T.. Interpretation of Ion-Exchange Chromatographic Retention Based on an Electrical Double-Layer Model. *Environ Sci Technol* 1998; **70**(9):1692–1700.
140. Pujar, N.S., Zydney, A.L.. Electrostatic effects on protein partitioning in size-exclusion chromatography and membrane ultrafiltration. *J Chromatogr A* 1998; **796**(2):229–238.
141. Tatárová, I., Drevenák, P., Kosior, A., Polakovič, M.. Equilibrium and kinetics of protein binding on ion-exchange cellulose membranes with grafted polymer layer. *Chem Pap* 2013; **67**(12):1–10.
142. Gagnon, P.. Technology trends in antibody purification. *J Chromatogr A* 2012; **1221**:57–70.
143. Riordan, W., Heilmann, S., Brorson, K., Seshadri, K., He, Y., Etzel, M.. Design of salt-tolerant membrane adsorbers for viral clearance. *Biotechnol Bioeng* 2009; **103**(5):920–929.
144. Napadensky, B., Shinkazh, O., Teella, A., Zydney, A.L.. Continuous Countercurrent Tangential Chromatography for Monoclonal Antibody Purification. *Sep Sci Technol* 2013; **48**(9):1289–1297.
145. Aumann, L., Morbidelli, M.. A continuous multicolumn countercurrent solvent gradient purification (MCSGP) process. *Biotechnol Bioeng* 2007; **98**(5):1043–1055.
146. Maranga, L., Rueda, P., Antonis, A.F.G., Vela, C., Langeveld, J.P.M., Casal, J.I., et al. Large scale production and downstream processing of a recombinant porcine parvovirus vaccine. *Appl Microbiol Biotechnol* 2002; **59**(1):45–50.
147. Elliott, P., Billingham, S., Bi, J., Zhang, H.. Quality by design for biopharmaceuticals: a historical review and guide for implementation. *Pharm Bioprocess* 2013; **1**(1):105–122.

148. Vicente, T., Mota, J.P.B., Peixoto, C., Alves, P.M., Carrondo, M.J.T.. Rational design and optimization of downstream processes of virus particles for biopharmaceutical applications: Current advances. *Biotechnol Adv* 2011; **29**(6):869–878.
149. Wiendahl, M., Schulze Wierling, P., Nielsen, J., Fomsgaard Christensen, D., Krarup, J., Staby, A., et al. High Throughput Screening for the Design and Optimization of Chromatographic Processes – Miniaturization, Automation and Parallelization of Breakthrough and Elution Studies. *Chem Eng Technol* 2008; **31**(6):893–903.
150. Schenauer, M.R., Flynn, G.C., Goetze, A.M.. Identification and quantification of host cell protein impurities in biotherapeutics using mass spectrometry. *Anal Biochem* 2012; **428**(2):150–157.
151. Berrill, A., Ho, S.V., Bracewell, D.G.. Mass spectrometry to describe product and contaminant adsorption properties for bioprocess development. *Biotechnol Bioeng* 2011; **108**(8):1862–1871.
152. Thompson, C.M., Petiot, E., Lennaertz, A., Henry, O., Kamen, A.A.. Analytical technologies for influenza virus-like particle candidate vaccines: challenges and emerging approaches. *Virol J* 2013; **10**(1):141.
153. Downard, K.M., Morrissey, B., Schwahn, A.B.. Mass spectrometry analysis of the influenza virus. *Mass Spectrom Rev* 2009; **28**(1):35–49.



# APPENDIX





Figure A1: Amount of the different filter aids used in dry state.

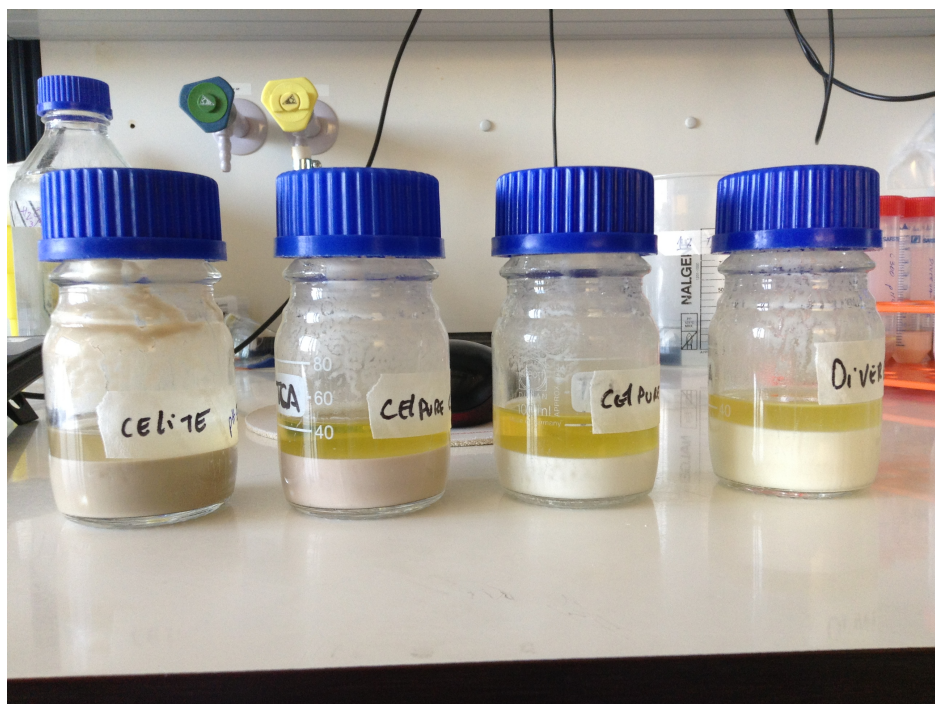


Figure A2: Volume filled by the wet filter aid with 50 mL of virus bulk after settling for 48 hours.